Generalized Compute-Compress-and-Forward

Hai Cheng, Xiaojun Yuan, *Senior Member, IEEE*, and Yihua Tan

***Abstract*— Compute-and-forward (CF) harnesses interference in wireless communications by exploiting structured coding. The key idea of CF is to compute integer combinations of code words from multiple source nodes, rather than to decode individual code words by treating others as noise. Compute-compress-and-forward (CCF) can further enhance the network performance by introducing compression operations at receivers. In this paper, we develop a more general compression framework, termed generalized CCF (GCCF), where the compression function involves the selection of message segments over finite fields. We show that GCCF achieves a broader compression rate region than CCF. We also compare our compression rate region with the fundamental Slepian–Wolf (SW) region. We show that GCCF is optimal in the sense of achieving the minimum total compression rate. We also establish the criteria under which GCCF achieves the SW region. In addition, we consider a two-hop relay network employing the GCCF scheme. We formulate a sum-rate maximization problem and develop an approximate algorithm to solve the problem. Numerical results are presented to demonstrate the performance superiority of GCCF over CCF and other schemes.**

***Index Terms*— Compute-and-forward, nested lattice codes, compute-compress-and-forward, distributed source coding.**

I. Introduction

COMPUTE-AND-FORWARD (CF) is an advanced relay technique that exploits structured coding to harness interference in wireless communications [1]. The key idea of CF is to suppress interference by computing integer combinations of source codewords, rather than decoding individual source codewords. CF employs nested lattice coding [2] to ensure that the computed integer combinations in CF are still valid codewords. A nested lattice codebook is formed by the set of lattice points of a coding lattice confined within the fundamental Voronoi region of a coarser shaping lattice.

Manuscript received March 20, 2017; revised December 10, 2017; accepted July 1, 2018. Date of publication August 10, 2018; date of current version December 19, 2018. H. Cheng and X. Yuan are supported in part by the National Nature Science Foundation of China under Grant 61471241 and in part by the China Recruitment Program of Global Young Experts. This paper was presented in part at the 2017 IEEE GLOBECOM.

H. Cheng is with the School of Information Science and Technology, ShanghaiTech University, Shanghai 201210, China (e-mail: chenghai@shanghaitech.edu.cn).

X. Yuan is with the National Key Laboratory of Science and Technology on Communication, Center for Intelligent Networking and Communications, University of Electronic Science and Technology of China, Chengdu 611731, China (e-mail: xjyuan@uestc.edu.cn).

Y. Tan was with the Department of Information Engineering, The Chinese University of Hong Kong, Hong Kong. He is now with NetEase Inc., Hangzhou 310000, China (e-mail: tanyihua@cuhk.edu.hk).

Communicated by J.-F. Chamberland, Associate Editor for Communications.

Color versions of one or more of the figures in this paper are available online at http://ieeexplore.ieee.org.

Digital Object Identifier 10.1109/TIT.2018.2864638

Since the advent of CF, many works followed up to enhance the throughput of CF-based relay networks [3]–[16]. In the original CF [1], all nested lattice codes share a common shaping lattice, and all transmitters are constrained by a same power budget. In [3]–[5], asymmetric CF allows asymmetric construction of shaping lattices and unequal power allocation across transmitters, so as to improve the computation performance. Nazer *et al.* [6], [7] studied successive computation of multiple codeword combinations to enlarge the achievable rate region of a receiver. Niesen and Whiting [8] studied the degrees of freedom of CF to characterize the behavior of CF in the high signal-to-noise ratio (SNR) regime.

Recently, Tan and Yuan [9] pointed out that, as the computed codewords in a CF-based multi-hop relay network are in general correlated, the performance of the network can be enhanced if the codewords computed at relays are further compressed to reduce the information redundancy. The corresponding relaying strategy is referred to as compute-compress-and-forward (CCF). In CCF, each relay processes its computed message by taking quantization and modulo (QM) operation over a pair of carefully selected nested lattices. Significant performance gains of CCF over CF have been demonstrated by the numerical results in [9]. However, as QM-based CCF is not necessarily optimal, it is desirable to push CCF towards its fundamental performance limit.

In this paper, we consider the efficient transceiver design for an interference channel with L transmitters and L receivers, where L is an arbitrary integer. We generalize CCF by allowing each receiver to compress its computed codeword by selecting a portion of message segments. We follow the linear labeling approach in [5] to realize the compression operation over finite fields, which involves much lower computational complexity than the QM operations in CCF. We show that the generalized CCF (GCCF) scheme can achieve a broader compression rate region than the original CCF in [9]. We also show that the compression problem can be interpreted as a distributed source-coding problem. Based on that, we compare the compression rate region of GCCF with the Slepian-Wolf region, where the latter is the optimal rate region for distributed source coding [17]. We show that GCCF, though in general cannot achieve the entire Slepian-Wolf region, is optimal in the sense of minimizing the total compression rate. Also, we prove that these two regions coincide in the following two cases: (i) the channel consists of only two transmitters and two receivers, i.e., $L = 2$; or (ii) all the transmitters share a common shaping lattice.

The proposed GCCF scheme, similar to CCF, can serve as a building block to construct a multi-hop relay network. In particular, we consider a two-hop relay network in which

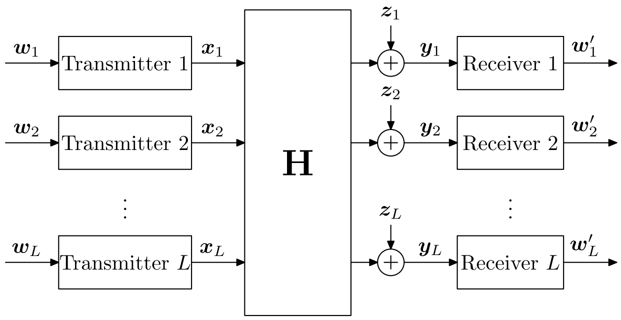

Fig. 1. An interference channel with L transmitters and L receivers.

a single destination node is required to recover all the messages from the sources. We establish an achievable rate region of the relay network and then formulate a mixed-integer-programing problem for sum-rate maximization. We show that the problem can be approximately solved based on Lenstra-Lenstra-Lovsz (LLL) lattice basis reduction [15], [16] and differential evolution [18]. Numerical results are presented to demonstrate the superiority of our proposed GCCF scheme over the other benchmark schemes including CCF.

The remainder of this paper is organized as follows. In Section II, we introduce the system model and the background of CCF. In Section III, we describe the proposed GCCF scheme. In Section IV, we derive the compression rate region of GCCF, and discuss its relation with the Slepian-Wolf region. In Section V, we first establish an achievable rate region of a multi-hop relay network based on GCCF, and then present an approximate algorithm to solve the sum-rate maximization problem of a two-hop GCCF network. Numerical results are also provided to show the performance superiority of GCCF. Finally, conclusions are presented in Section VI.

II. Preliminaries

A. System Model

Consider an interference channel with L transmitters and L receivers, as illustrated in Fig. 1. Each transmitter or receiver node is equipped with a single antenna. The message of transmitter l is a vector $\boldsymbol{w}_l \in \mathbb{Z}_q^{b_l}$, where q is a prime number, and $\mathbb{Z}_q = \{0, 1, \cdots, p-1\}$ is a prime field. Transmitter l encodes message $\boldsymbol{w}_l$ into $\boldsymbol{x}_l \in \mathbb{R}^{n\times 1}$ and then transmits $\boldsymbol{x}_l$ to the receivers over an additive white Gaussian noise (AWGN) channel. Each receiver m observes an output signal

$$\boldsymbol{y}_m = \sum_{l=1}^{L} h_{ml}\boldsymbol{x}_l + \boldsymbol{z}_m, \quad \text{for } m \in \mathcal{I}_L \tag{1}$$

where $h_{ml} \in \mathcal{N}(0,1)$ is the channel coefficient of the link from source l to relay m, $\boldsymbol{z}_m \in \mathbb{R}^{n\times 1}$ is a Gaussian noise vector drawn from $\mathcal{N}(\mathbf{0}, \boldsymbol{I}_n)$ with $\boldsymbol{I}_n$ being the n-by-n identity matrix, and $\mathcal{I}_l$ denotes the index set of integers from 1 to l and $\mathcal{I}_0 = \emptyset$. Denote by $\boldsymbol{H} = [\boldsymbol{h}_1, \boldsymbol{h}_2, \cdots, \boldsymbol{h}_L]^{\mathrm{T}}$ the channel matrix, where $\boldsymbol{h}_m = [h_{m1}, h_{m2}, \cdots, h_{mL}]^{\mathrm{T}}$ is the channel vector seen by receiver m. The average power of transmitter l is $p_l = \frac{1}{n}\mathrm{E}\|\boldsymbol{x}_l\|^2$ satisfying $p_l \le P_l$, where P_l is the power budget of transmitter l. We assume full channel state information, i.e., all the channel coefficients are perfectly known.

The CCF scheme in [9] can be applied to the channel model in (1). In CCF, each transmitter encodes its message by a nested lattice code and then sends the codeword to the receivers. Each receiver computes an integer linear combination of the nested lattice codewords from the received signal, and then compresses the computed codeword. The goal of the compression operation is to reduce the forwarding rates of the receivers in relaying, so as to improve the spectrum efficiency of the relay network. In this paper, we aim to generalize the compression operation in CCF for more efficient forwarding.

B. Nested Lattice Codes

We start with a brief introduction of nested lattice coding. A lattice $\Lambda \subset \mathbb{R}^n$ is a discrete group with the following property. If $\boldsymbol{t}_1 \in \Lambda$ and $\boldsymbol{t}_2 \in \Lambda$, then $\boldsymbol{t}_1 + \boldsymbol{t}_2 \in \Lambda$; and if $\boldsymbol{t}_1 \in \Lambda$, then $-\boldsymbol{t}_1 \in \Lambda$. A lattice can be represented as

$$\Lambda = \{\boldsymbol{s} = \boldsymbol{G}\boldsymbol{c} : \boldsymbol{c} \in \mathbb{Z}^{n\times 1}\} \tag{2}$$

where $\boldsymbol{G} \in \mathbb{R}^{n\times n}$ is the generator matrix of Λ. The quantization of $\boldsymbol{x} \in \mathbb{R}^n$ on Λ is the nearest lattice point to $\boldsymbol{x}$ in Λ, i.e.

$$\boldsymbol{Q}_\Lambda(\boldsymbol{x}) = \arg\min_{\boldsymbol{t}\in\Lambda} \|\boldsymbol{t} - \boldsymbol{x}\| \tag{3}$$

where $\|\cdot\|$ denotes the l_2 norm of a vector. The quantization error is given by

$$\boldsymbol{x} \bmod \Lambda = \boldsymbol{x} - Q_\Lambda(\boldsymbol{x}) \tag{4}$$

where "mod" represents the modulo operation. The fundamental Voronoi region of Λ is defined by

$$\mathcal{V} = \{\boldsymbol{x} \in \mathbb{R}^n : Q_\Lambda(\boldsymbol{x}) = \mathbf{0}\}. \tag{5}$$

The second moment of Λ is defined by

$$\sigma_\Lambda^2 = \frac{1}{n}\int_{\mathcal{V}} \frac{\|\boldsymbol{x}\|^2}{\mathrm{Vol}(\mathcal{V})} d\boldsymbol{x} \tag{6}$$

where $\mathrm{Vol}(\mathcal{V})$ is the volume of $\mathcal{V}$. The normalized second moment of Λ is defined by

$$G(\Lambda) = \frac{\sigma_\Lambda^2}{(\mathrm{Vol}(\mathcal{V}))^{\frac{2}{n}}}. \tag{7}$$

If $\Lambda_1 \subseteq \Lambda_2$, we say that Λ_1 is nested in Λ_2 and that Λ_1 is coarser than Λ_2 (or alternatively, Λ_2 is finer than Λ_1). An example of a pair of nested lattices is given in Fig. 2. We construct a lattice codebook $\mathcal{C}$ based on a nested lattice pair (Λ_s, Λ_c) satisfying $\Lambda_s \subseteq \Lambda_c$, where Λ_s is the shaping lattice and Λ_c is the coding lattice. Denote by $\mathcal{V}_s$ and $\mathcal{V}_c$ the fundamental Voronoi regions of Λ_s and Λ_c, respectively. The lattice codebook $\mathcal{C}$ can be represented as

$$\mathcal{C} = \Lambda_c \bmod \Lambda_s = \Lambda_c \cap \mathcal{V}_s. \tag{8}$$

The rate of $\mathcal{C}$ is given by

$$R = \frac{1}{n}\log|\mathcal{C}| = \frac{1}{n}\log\frac{\mathrm{Vol}(\mathcal{V}_s)}{\mathrm{Vol}(\mathcal{V}_c)} \tag{9}$$

where log denotes logarithm with base 2.

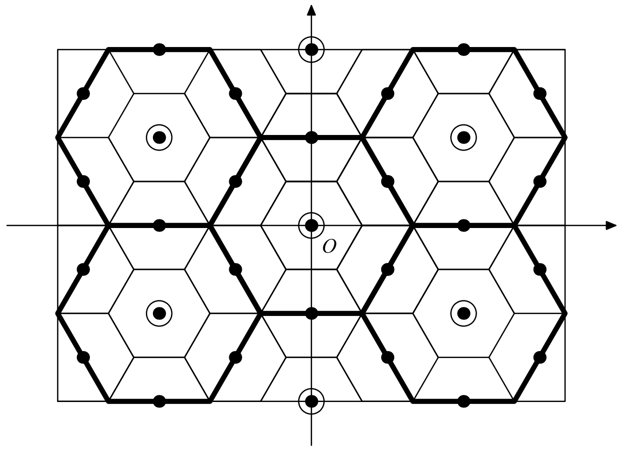

Fig. 2. An illustration of a nested lattice pair (Λ_s, Λ_c) satisfying $\Lambda_s \subset \Lambda_c \subset \mathbb{R}^2$. Black points "•" are elements of the coding lattice Λ_c and the black circles "◯" are elements of the shaping lattice Λ_s. The Voronoi regions of Λ_c and Λ_s are hexagons with thin and thick edges, respectively. The nested lattice codebook consists of the set of all fine lattice points in the fundamental Voronoi region of the coarse lattice.

C. Encoding at Transmitters

We now describe the encoding at the transmitters. We employ the lattice construction method in [5] to construct a chain of $2L$ nested lattices $\Lambda_1, \Lambda_2, \cdots, \Lambda_{2L}$ as follows.

Let $i_1, i_2, \cdots, i_{2L}$ be integers satisfying $0 \le i_1 \le i_2 \le \cdots \le i_{2L}$. Consider a matrix $\boldsymbol{G} \in \mathbb{Z}_q^{n \times i_{2L}}$ with i.i.d elements uniformly drawn over $\mathbb{Z}_q$. Let $\boldsymbol{G}_k$ be the matrix consisting of the first i_k columns of $\boldsymbol{G}$, for $k = 1, 2, \cdots, 2L$. Define $\mathcal{D}_k$ to be the discrete codebook generated by $\boldsymbol{G}_k$:

$$\mathcal{D}_k = \left\{ \boldsymbol{x} \in \mathbb{Z}_q^n : \boldsymbol{x} = (\boldsymbol{G}_k \boldsymbol{w}) \bmod q, \boldsymbol{w} \in \mathbb{Z}_q^{i_k} \right\}. \quad (10)$$

Define the mapping $\phi : \mathbb{Z}_q \to \mathbb{R}$ as

$$\phi(x) \triangleq \gamma q^{-1} x, \quad (11)$$

where $\gamma \in \mathbb{R}^{++}$ is a constant coefficient. The corresponding inverse map is given by

$$\bar{\phi}(x) = (\gamma^{-1} q x) \bmod q \quad (12)$$

where $x \in \gamma q^{-1}\mathbb{Z}$. These mapping functions operate elementwise when applied to vectors. Following lattice Construction A [2], we create the lattice

$$\Lambda_k = \left\{ \boldsymbol{t} \in \gamma q^{-1} \mathbb{Z}^n : \bar{\phi}(\boldsymbol{t}) \in \mathcal{D}_{i_k} \right\}. \quad (13)$$

We see that $\boldsymbol{t} \in \Lambda_k$ if and only if $\bar{\phi}(\boldsymbol{t}) \in \mathcal{D}_{i_k}$. We refer to $\bar{\phi}(\boldsymbol{t})$ as the corresponding *linear codeword* of $\boldsymbol{t}$. Since $\mathcal{D}_{i_1} \subseteq \mathcal{D}_{i_2} \subseteq \cdots \subseteq \mathcal{D}_{i_{2L}}$, the constructed lattices are nested as $\Lambda_1 \subseteq \Lambda_2 \subseteq \cdots \subseteq \Lambda_{2L}$. Following the settings of $n, p, \gamma, \{i_k\}$ in [5], we construct the nested lattices chain $\Lambda_1 \subseteq \Lambda_2 \subseteq \cdots \subseteq \Lambda_{2L}$, where $\{\Lambda_k\}$ satisfy any given second moments $\{\sigma^2_{\Lambda_k}\}$ and are simultaneously good for AWGN and good for MSE quantization [19].

For each source l, we choose a lattice pair $(\Lambda_{\mathrm{s},l}, \Lambda_{\mathrm{c},l})$ from the nested lattice chain to construct a lattice codebook

$$\mathcal{C}_l = \Lambda_{\mathrm{c},l} \cap \mathcal{V}_{\mathrm{s},l}. \quad (14)$$

Let $\pi_s(\cdot)$ be a permutation satisfying $\Lambda_{s,\pi_s(1)} \subseteq \Lambda_{s,\pi_s(2)} \subseteq \cdots \subseteq \Lambda_{s,\pi_s(L)}$, which gives the nested order of L shaping lattices. Denote by $\pi(\cdot)$ the lattice chain permutation that is a bijective map from $\{1, \cdots, 2L\}$ to $\{1, \cdots, 2L\}$ satisfying

$$\Lambda_{\pi(2l-1)} \subseteq \Lambda_{\pi(2l)}, \quad l \in \mathcal{I}_L. \quad (15)$$

With (15), we construct each $\mathcal{C}_l$ using the lattice pair $(\Lambda_{\pi(2l-1)}, \Lambda_{\pi(2l)})$, $l \in \mathcal{I}_L$. This implies the following relation:

$$l = \left\lceil \frac{\pi^{-1}(k)}{2} \right\rceil, \quad 1 \le k \le 2L. \quad (16)$$

From (16), if $\pi^{-1}(k)$ is even, then $\Lambda_k = \Lambda_{\mathrm{c},l}$ with $l = \frac{\pi^{-1}(k)}{2}$; otherwise, $\Lambda_k = \Lambda_{\mathrm{s},l}$ with $l = \frac{\pi^{-1}(k)+1}{2}$.

The message $\boldsymbol{w}_l$ of transmitter l is uniformly drawn from $\mathbb{Z}_q^{b_l}$ with $b_l = i_{\pi(2l)} - i_{\pi(2l-1)}$. The message $\boldsymbol{w}_l$ is encoded into a lattice codeword $\boldsymbol{t}_l \in \mathcal{C}_l$ as follows. We zero-pad $\boldsymbol{w}_l$ with $i_{\pi(2l-1)}$ leading zeros and $i_{2L} - i_{\pi(2l)}$ trailing zeros. The zero-padded vector is mapped onto a lattice codeword $\boldsymbol{t}_l$ in $\mathcal{C}_l$:

$$\boldsymbol{t}_l = \left(\gamma q^{-1} \left(\left(\boldsymbol{G} \left[\boldsymbol{0}^{\mathrm{T}}_{i_{\pi(2l-1)}}, \boldsymbol{w}_l^{\mathrm{T}}, \boldsymbol{0}^{\mathrm{T}}_{i_{2L} - i_{\pi(2l)}} \right]^{\mathrm{T}} \right) \bmod q \right) \right) \bmod \Lambda_{\mathrm{s},l}, \quad l \in \mathcal{I}_L. \quad (17)$$

By following the proof of [1, Lemma 5], it can be shown that the mapping in (17) is an isomorphism between $\mathbb{Z}_q^{b_l}$ and $\mathcal{C}_l$. Thus, $\boldsymbol{t}_l$ is uniformly distributed over $\mathcal{C}_l$. The rate of source l is given by

$$r_l = \frac{1}{n} \log |\mathcal{C}_l| = \frac{1}{n} \log \frac{\mathrm{Vol}(\mathcal{V}_{\mathrm{s},l})}{\mathrm{Vol}(\mathcal{V}_{\mathrm{c},l})}. \quad (18)$$

From the isomorphism between $\mathbb{Z}_q^{b_l}$ and $\mathcal{C}_l$, r_l can be rewritten by

$$r_l = \frac{1}{n} \log q^{b_l} = \frac{i_{\pi(2l)} - i_{\pi(2l-1)}}{n} \log q. \quad (19)$$

Following the approach in [4], we construct the channel input vector of transmitter l as

$$\boldsymbol{x}_l = (\boldsymbol{t}_l / \beta_l - \boldsymbol{d}_l) \bmod \Lambda_{\mathrm{s},l}/\beta_l \quad (20)$$

where $\beta_l \in \mathbb{R}$ is a scaling factor, and $\boldsymbol{d}_l$ is a random dithering signal uniformly distributed over the scaled Voronoi region $\mathcal{V}_{\mathrm{s},l}/\beta_l$. From the Crypto lemma [2], $\boldsymbol{x}_l$ is independent of $\boldsymbol{t}_l$ and is uniformly distributed over $\mathcal{V}_{\mathrm{s},l}/\beta_l$ [2]. We note that $\{\beta_l\}$ are set as $\beta_l = 1, l \in \mathcal{I}_L$ in the original CCF scheme in [9]. Here we treat $\{\beta_l\}$ as system variables to be optimized.

From (6) and (7), the average power of $\boldsymbol{x}_l$ is given by

$$p_l = \frac{1}{n} \mathrm{E} \|\boldsymbol{x}_l\|^2 = \frac{1}{n} \int_{\mathcal{V}_{\mathrm{s},l}/\beta_l} \frac{\|\boldsymbol{x}\|^2}{\mathrm{Vol}(\mathcal{V}_{\mathrm{s},l}/\beta_l)} d\boldsymbol{x}$$
$$= G(\Lambda_{\mathrm{s},l}/\beta_l) \left(\mathrm{Vol}(\mathcal{V}_{\mathrm{s},l}/\beta_l) \right)^{\frac{2}{n}}. \quad (21)$$

As $\Lambda_{\mathrm{s},l}/\beta_l$ is good for MSE quantization, we obtain $\lim_{n \to \infty} G(\Lambda_{\mathrm{s},l}/\beta_l) = \frac{1}{2\pi e}$ [2]. Then, we have the following relation:

$$\mathrm{Vol}(\mathcal{V}_{\mathrm{s},l}) = \mathrm{Vol}(\mathcal{V}_{\mathrm{s},l}/\beta_l) \beta_l^n = \left(\frac{p_l \beta_l^2}{G(\Lambda_{\mathrm{s},l}/\beta_l)} \right)^{\frac{n}{2}}. \quad (22)$$

This implies that $\sigma^2_{\Lambda_{\mathrm{s},l}} = p_l \beta_l^2$ and the nesting order of $\{\Lambda_{\mathrm{s},l}\}$ is determined by the order of $\{p_l \beta_l^2\}$.

D. Computation at Receivers

Upon receiving $\boldsymbol{y}_m$ in (1), receiver m attempts to decodes an integer-linear combination from $\boldsymbol{y}_m$, denoted by

$$\boldsymbol{v}_m = \left(\sum_{l=1}^{L} a_{ml} (\boldsymbol{t}_l - Q_{\Lambda_{\mathrm{s},l}}(\boldsymbol{t}_l - \beta_l \boldsymbol{d}_l)) \right) \bmod \Lambda_1. \quad (23)$$

The details of the decoding procedure follow the CF approach in [1]. Receiver m first multiplies $\boldsymbol{y}_m$ by α_m and then cancels the dithering signals, yielding

$$\begin{aligned} \boldsymbol{s}_m &= \alpha_m \boldsymbol{y}_m + \sum_{l=1}^{L} a_{ml} \beta_l \boldsymbol{d}_l \\ &\overset{(a)}{=} \sum_{l=1}^{L} a_{ml} \beta_l (\boldsymbol{t}_l/\beta_l - Q_{\Lambda_{\mathrm{s},l}/\beta_l}(\boldsymbol{t}_l/\beta_l - \boldsymbol{d}_l)) + \boldsymbol{z}'_m \\ &\overset{(b)}{=} \sum_{l=1}^{L} a_{ml} (\boldsymbol{t}_l - Q_{\Lambda_{\mathrm{s},l}}(\boldsymbol{t}_l - \beta_l \boldsymbol{d}_l)) + \boldsymbol{z}'_m \end{aligned} \quad (24)$$

where a_{ml} is an integer coefficient, and $\boldsymbol{z}'_m \triangleq \sum_{l=1}^{L} (\alpha_m h_{ml} - a_{ml}\beta_l)\boldsymbol{x}_l + \alpha_m \boldsymbol{z}_m$. In the above, step (a) follows from (1) and (20), and step (b) follows by noting $Q_\Lambda(\beta \boldsymbol{t}) = \beta Q_{\Lambda/\beta}(\boldsymbol{t})$ for $\beta > 0$. Then, receiver m quantizes $\boldsymbol{s}_m$ over $\Lambda_{f,m}$ and takes modulo over the coarsest lattice Λ_1, yielding

$$\begin{aligned} \hat{\boldsymbol{v}}_m &= Q_{\Lambda_{f,m}}(\boldsymbol{s}_m) \bmod \Lambda_1 \\ &= Q_{\Lambda_{f,m}}\left(\sum_{l=1}^{L} a_{ml} \big(\boldsymbol{t}_l - Q_{\Lambda_{\mathrm{s},l}}(\boldsymbol{t}_l - \beta_l \boldsymbol{d}_l) \big) + \boldsymbol{z}'_m \right) \bmod \Lambda_1 \end{aligned} \quad (25)$$

where $\Lambda_{f,m}$ is the finest lattice among $\{\Lambda_{\mathrm{c},l}\}_1^L$ with $a_{ml} \neq 0$.

We say that a rate tuple $(r_1, r_2, \cdots, r_L)$ is achievable if

$$\lim_{n \to \infty} \Pr\{\hat{\boldsymbol{v}}_m \neq \boldsymbol{v}_m\} = 0, \quad \text{for } m \in \mathcal{I}_L. \quad (26)$$

Based on the results in [4] and [9], the rate tuple $(r_1, r_2, \cdots, r_L)$ is achievable if for $l \in \mathcal{I}_L$,

$$r_l < \frac{1}{2} \log^+ \left\{ \min_{m: a_{ml} \neq 0} \frac{p_l \beta_l^2}{\| \boldsymbol{P}^{\frac{1}{2}} \tilde{\boldsymbol{a}}_m \|^2 - \frac{(\boldsymbol{h}_m^{\mathrm{T}} \boldsymbol{P} \tilde{\boldsymbol{a}}_m)^2}{1 + \| \boldsymbol{P}^{\frac{1}{2}} \boldsymbol{h}_m \|^2}} \right\} \triangleq \hat{r}_l \quad (27)$$

where $\boldsymbol{P} = \mathrm{diag}\{p_1, p_2, \cdots, p_L\}$ and $\tilde{\boldsymbol{a}}_m = [\beta_1 \; a_{m1}, \beta_2 \; a_{m2}, \cdots, \beta_L a_{mL}]^{\mathrm{T}}$. Denote by $\boldsymbol{A}$ the integer coefficient matrix with the (m, l)-th element given by a_{ml}. Following [1], we always assume $\boldsymbol{A}$ is invertible over $\mathbb{Z}_q^{L \times L}$, so that $\{\boldsymbol{t}_l\}_1^L$ can be recovered from $\{\boldsymbol{v}_m\}_1^L$. An achievable rate region is then given by

$$\mathcal{R}_{\mathrm{cpu}} = \left\{ (r_1, r_2, \cdots, r_L) \in \mathbb{R}_+^L | r_l \leq \hat{r}_l, l \in \mathcal{I}_L \right\}. \quad (28)$$

We refer to the rate region in (28) as the computation rate region. Here we use shorthand "cpu" for computation.

TABLE I

FREQUENTLY USED NOTATION

Notation	Definition
$\boldsymbol{w}_l$	The message of the l-th source
$\boldsymbol{t}_l$	Lattice codeword of the l-th source
$\boldsymbol{x}_l$	Transmitted signal of the l-th source
$\boldsymbol{\Lambda}_k$	The k-th lattice on the lattice chain
$\Lambda_{\mathrm{c},l}$	Coding lattice of the l-th source
$\Lambda_{\mathrm{s},l}$	Shaping lattice of the l-th source
$\pi(\cdot)$	A permutation of lattice chain satisfying $\Lambda_{\pi(2l-1)} = \Lambda_{\mathrm{s},l}$ and $\Lambda_{\pi(2l)} = \Lambda_{\mathrm{c},l}$
$\pi_{\mathrm{s}}(\cdot)$	A permutation satisfying $\Lambda_{\mathrm{s},\pi_{\mathrm{s}}(1)} \subseteq \Lambda_{\mathrm{s},\pi_{\mathrm{s}}(2)} \subseteq \cdots \subseteq \Lambda_{\mathrm{s},\pi_{\mathrm{s}}(L)}$
$\pi_{\mathrm{c}}(\cdot)$	A permutation satisfying $\Lambda_{\mathrm{c},\pi_{\mathrm{c}}(1)} \subseteq \Lambda_{\mathrm{c},\pi_{\mathrm{c}}(2)} \subseteq \cdots \subseteq \Lambda_{\mathrm{c},\pi_{\mathrm{c}}(L)}$
$Q_\Lambda(\boldsymbol{x})$	Quantization of $\boldsymbol{x}$ over lattice Λ
$\boldsymbol{x} \bmod \Lambda$	$\boldsymbol{x}$ modulo Λ
$\mathcal{V}$	Fundamental Voronoi region of a lattice
$\mathrm{Vol}(\mathcal{V})$	Volume of $\mathcal{V}$
β_l	Precoding coefficient at the l-th source.
$\mathbf{A}$	Linear combination matrices $\boldsymbol{A} \in \mathbb{R}^{L \times M}$
$\mathbf{A}(\mathcal{S}, \mathcal{S}')$	Submatrix of $\boldsymbol{A}$ with rows indexed by $\mathcal{S}$ and the columns indexed by $\mathcal{S}'$
$\|\mathcal{S}\|$	Cardinality of $\mathcal{S}$
$\mathrm{rank}(\boldsymbol{A})$	Rank of matrix $\boldsymbol{A}$
r_l	Transmission rate of the l-th source
R_m	Forwarding rate of the m-th receiver
$\boldsymbol{v}_m$	Computed codeword at receiver m
$\boldsymbol{\delta}_m$	Compressed codeword at receiver m
$\mathcal{R}_{\mathrm{cpu}}$	Computation rate region in (28)
$\mathcal{R}_{\mathrm{cpr}}$	Compression rate region in (78)
$\varphi(\cdot)$	The linear labeling function
$\boldsymbol{w}_{l,k}$	The k-th message segment of $\varphi(\boldsymbol{t}_l)$
$\boldsymbol{u}_{m,k}$	The k-th message segment of $\varphi(\boldsymbol{v}_m)$
$r_{\mathrm{v},k}$	Entropy rate of k-th message segment
$\mathcal{I}_l$	Index set $\{1, 2, \cdots, l\}$
α_m	Weight coefficient of R_m in (75a)
$\pi_\alpha(\cdot)$	Permutation defined by the order of $\{\alpha_m\}$

E. Compression at Receivers

From (25), $\{\hat{\boldsymbol{v}}_m\}$ computed at receivers are generally correlated, as they are constructed by the same set of $\{\boldsymbol{t}_l\}$. Recall that each receiver in the channel model (1) serves as a relay node. Forwarding $\{\hat{\boldsymbol{v}}_m\}$ directly at the receivers may lead to spectral inefficiency. That is, each receiver m needs to compress $\hat{\boldsymbol{v}}_m$, so as to reduce the forwarding rate [9], [20]. Specifically, the compression at receiver m is to generate a mapping from $\hat{\boldsymbol{v}}_m$ to $\hat{\boldsymbol{\delta}}_m$

$$\hat{\boldsymbol{\delta}}_m = \psi_m(\hat{\boldsymbol{v}}_m) \quad (29)$$

at a reduced rate $R_m(\leq r_m)$, where $\psi_m(\cdot)$ is referred to as the compression function of receiver m. For the overall scheme, the compression is required to be information lossless, i.e., $\{\hat{\boldsymbol{v}}_m\}_1^L$ can be exactly recovered from $\{\hat{\boldsymbol{\delta}}_m\}_1^L$. We say that a compression rate tuple $(R_1, R_2, \cdots, R_L)$ is achievable if $\{\hat{\boldsymbol{v}}_m\}_1^L$ can be recovered from $\{\hat{\boldsymbol{\delta}}_m\}_1^L$ without distortion. The convex hull of all achievable compression rate tuples gives the *compression rate region*, denoted by $\mathcal{R}_{\mathrm{cpr}}$. For convenience of discussion, we henceforth assume that there is no error in receiver computations, i.e., $\hat{\boldsymbol{v}}_m = \boldsymbol{v}_m$ for $m \in \mathcal{I}_L$. Correspondingly, the error-free version of $\hat{\boldsymbol{\delta}}_m$ is denoted by $\boldsymbol{\delta}_m$. Before proceeding to the next section, we list some frequently used notations in Table I.

III. Proposed Compression Scheme

We first describe a technique termed *linear labeling* [5], [21] which conveniently connects the nested lattice codewords to messages over finite fields. The proposed compression scheme can be viewed as a process of selecting "useful" message segments. Finally, we discuss the relation between the proposed scheme and the original CCF in [9].

A. Linear Labeling

We now introduce the concept of *linear labeling* [5], [21]. A mapping $\varphi : \Lambda_{2L} \to \mathbb{Z}_q^{i_{2L}-i_1}$ from lattice points in Λ_{2L} to message vectors in $\mathbb{Z}_q^{i_{2L}-i_1}$ is called a *linear labeling* if it satisfies the following two conditions:

(i) The last $i_{2L} - i_k$ elements of $\varphi(\boldsymbol{t})$ are zeros if and only if the lattice point $\boldsymbol{t} \in \Lambda_k$;

(ii) For all $a_l \in \mathbb{Z}$ and $\boldsymbol{t}_l \in \Lambda_{2L}$, we have $\varphi\left(\sum_{l=1}^{L} a_l \boldsymbol{t}_l\right) = \left(\sum_{l=1}^{L}(a_l \bmod q)\varphi(\boldsymbol{t}_l)\right) \bmod q$.

Lemma 1: Assume that $\boldsymbol{G}$ is full rank. Let $\varphi : \Lambda_{2L} \to \mathbb{Z}_q^{i_{2L}-i_1}$ be a function that maps each $\boldsymbol{t} \in \Lambda_{2L}$ to the vector $\varphi(\boldsymbol{t})$ which consists of the last $i_{2L} - i_1$ elements of vector $\boldsymbol{c}$ satisfying $\bar{\phi}(\boldsymbol{t}) = (\boldsymbol{G}\boldsymbol{c}) \bmod q$. Then, $\varphi(\cdot)$ is a linear labeling.

Lemma 1 is proved in [5, Appendix G]. In the following, we always assume that φ is the liner labeling function given in Lemma 1. Note that the encoding function in (17) can be rewritten as

$$\boldsymbol{t}_l = \left(\phi\left(\left(\boldsymbol{G}\left[\boldsymbol{0}_{i_1}^{\mathrm{T}}, \tilde{\boldsymbol{w}}_l^{\mathrm{T}}\right]^{\mathrm{T}}\right) \bmod q\right)\right) \bmod \Lambda_{\mathrm{s},l}, \tag{30}$$

where

$$\tilde{\boldsymbol{w}}_l = \left[\boldsymbol{0}_{i_{\pi(2l-1)}-i_1}^{\mathrm{T}}, \boldsymbol{w}_l^{\mathrm{T}}, \boldsymbol{0}_{i_{2L}-i_{\pi(2l)}}\right]^{\mathrm{T}} \in \mathbb{Z}_q^{i_{2L}-i_1}. \tag{31}$$

Define an inverse operation $\bar{\varphi}(\cdot) : \mathbb{Z}_q^{i_{2L}-i_1} \to \Lambda_{2L}$ for $\varphi(\cdot)$:

$$\bar{\varphi}(\boldsymbol{w}) = \phi\left(\left(\boldsymbol{G}\left[\boldsymbol{0}_{i_1}^{\mathrm{T}}, \boldsymbol{w}^{\mathrm{T}}\right]^{\mathrm{T}}\right) \bmod q\right). \tag{32}$$

Then,

$$\varphi\left(\bar{\varphi}(\boldsymbol{w})\right) = \boldsymbol{w}, \tag{33}$$

and (17) can be rewritten as

$$\boldsymbol{t}_l = \bar{\varphi}(\tilde{\boldsymbol{w}}_l) \bmod \Lambda_{\mathrm{s},l}. \tag{34}$$

Lemma 2: The linear labeling $\varphi(\cdot)$ given in Lemma 1 is a bijection between $\Lambda_{2L} \cap \mathcal{V}_1$ and $\mathbb{Z}_q^{i_{2L}-i_1}$.

The proof of Lemma 2 is given in Appendix A. With linear labeling, it is convenient to analyze the correlation between the computed codewords $\{\boldsymbol{v}_l\}$ in the finite-field representation.

B. Label Splitting for Lattice Codeword

In this subsection, we consider splitting the label of each computed codewords $\boldsymbol{v}_m$ (a vector with length $i_{2L} - i_1$) into shorter vectors, termed *message segments*. Our proposed compression scheme is based on analyzing the correlation between those message segments.

Rewrite $\boldsymbol{v}_m$ in (23) as

$$\boldsymbol{v}_m = \left(\sum_{l=1}^{L} a_{ml}\tilde{\boldsymbol{t}}_l\right) \bmod \Lambda_1 \tag{35}$$

where

$$\tilde{\boldsymbol{t}}_l = \boldsymbol{t}_l - Q_{\Lambda_{\mathrm{s},l}}(\boldsymbol{t}_l - \beta_l \boldsymbol{d}_l). \tag{36}$$

From the definition of $\varphi(\cdot)$, the label of $\boldsymbol{v}_m$ is given by

$$\varphi(\boldsymbol{v}_m) = \left(\varphi(\sum_{l=1}^{L} a_{m,l}\tilde{\boldsymbol{t}}_l) - \varphi(Q_{\Lambda_1}(\sum_{l=1}^{L} a_{m,l}\tilde{\boldsymbol{t}}_l))\right) \bmod q \tag{37a}$$

$$= \left(\sum_{l=1}^{L}(a_{m,l} \bmod q)\varphi(\tilde{\boldsymbol{t}}_l)\right) \bmod q \tag{37b}$$

where $\varphi(Q_{\Lambda_1}(\sum_{l=1}^{L} a_{m,l}\tilde{\boldsymbol{t}}_l))$ in (37a) is equal to $\boldsymbol{0}$ since it is the label of a lattice point in Λ_1. As $\varphi(\boldsymbol{v}_m)$ is a linear combination of $\varphi(\tilde{\boldsymbol{t}}_l)$, to analyze the correlation between $\{\varphi(\boldsymbol{v}_m)\}$, it is helpful to first look into the elements in $\{\varphi(\tilde{\boldsymbol{t}}_l)\}$.

From (36), $\varphi(\tilde{\boldsymbol{t}}_l)$ can be rewritten as

$$\varphi(\tilde{\boldsymbol{t}}_l) = \left(\varphi(\boldsymbol{t}_l) - \varphi(Q_{\Lambda_{\mathrm{s},l}}(\boldsymbol{t}_l - \beta_l \boldsymbol{d}_l))\right) \bmod q, \tag{38}$$

where $Q_{\Lambda_{\mathrm{s},l}}(\boldsymbol{t}_l - \beta_l \boldsymbol{d}_l)$ is termed the *residual dither signal*. Since $Q_{\Lambda_{\mathrm{s},l}}(\boldsymbol{t}_l - \beta_l \boldsymbol{d}_l)$ is a lattice point in $\Lambda_{\mathrm{s},l}$, the last $i_{2L} - i_{\pi(2l-1)}$ elements of $\varphi(Q_{\Lambda_{\mathrm{s},l}}(\boldsymbol{t}_l - \beta_l \boldsymbol{d}_l))$ are all zeros and the non-zero elements locate at the first $i_{\pi(2l-1)} - i_1$ positions. Thus, $\varphi(\tilde{\boldsymbol{t}}_l)$ coincides with $\tilde{\boldsymbol{w}}_l$ in the last $i_{2L} - i_{\pi(2l-1)}$ elements.

To describe the message segments of $\varphi(\tilde{\boldsymbol{t}}_l)$, we first consider the message segments of $\varphi(\boldsymbol{t}_l)$ and $\varphi(Q_{\Lambda_{\mathrm{s},l}}(\boldsymbol{t}_l - \beta_l \boldsymbol{d}_l))$. The k-th message segment of $\varphi(\boldsymbol{t}_l)$ is defined as a vector over $\mathbb{Z}_q^{i_{k+1}-i_k}$, consisting of the $(i_k - i_1 + 1)$-th to $(i_{k+1} - i_1)$-th elements of $\varphi(\boldsymbol{t}_l)$. Thus, the label $\varphi(\boldsymbol{t}_l) \in \mathbb{Z}_q^{i_{2L}-i_1}$ can be generally split into $2L - 1$ message segments. Denote by $\boldsymbol{w}_{l,k}$ the k-th message segment of $\varphi(\boldsymbol{t}_l)$. Let the zero-padded $\boldsymbol{w}_{l,k}$ be

$$\tilde{\boldsymbol{w}}_{l,k} = \left[\boldsymbol{0}_{i_k-i_1}^{\mathrm{T}}, \boldsymbol{w}_{l,k}^{\mathrm{T}}, \boldsymbol{0}_{i_{2L}-i_{k+1}}^{\mathrm{T}}\right]^{\mathrm{T}} \in \mathbb{Z}_q^{i_{2L}-i_1}. \tag{39}$$

Then, $\varphi(\boldsymbol{t}_l)$ can be represented as

$$\varphi(\boldsymbol{t}_l) = \left(\sum_{k=1}^{2L-1} \tilde{\boldsymbol{w}}_{l,k}\right) \bmod q. \tag{40}$$

Further, by taking linear labeling on the both sides of (34), we obtain

$$\varphi(\boldsymbol{t}_l) = \varphi\left(\bar{\varphi}(\tilde{\boldsymbol{w}}_l) - Q_{\Lambda_{\mathrm{s},l}}\left(\bar{\varphi}(\tilde{\boldsymbol{w}}_l)\right)\right) \tag{41a}$$

$$= \left(\varphi\left(\bar{\varphi}(\tilde{\boldsymbol{w}}_l)\right) - \varphi\left(Q_{\Lambda_{\mathrm{s},l}}\left(\bar{\varphi}(\tilde{\boldsymbol{w}}_l)\right)\right)\right) \bmod q \tag{41b}$$

$$= \left(\tilde{\boldsymbol{w}}_l - \varphi\left(Q_{\Lambda_{\mathrm{s},l}}\left(\bar{\varphi}(\tilde{\boldsymbol{w}}_l)\right)\right)\right) \bmod q. \tag{41c}$$

Since $Q_{\Lambda_{\mathrm{s},l}}\left(\bar{\varphi}(\tilde{\boldsymbol{w}}_l)\right) \in \Lambda_{\mathrm{s},l}$, the last $i_{2L} - i_{\pi(2l-1)}$ elements of $\varphi\left(Q_{\Lambda_{\mathrm{s},l}}\left(\bar{\varphi}(\tilde{\boldsymbol{w}}_l)\right)\right)$ are zeros. Then, $\varphi(\boldsymbol{t}_l)$ coincides with $\tilde{\boldsymbol{w}}_l$ in the last $i_{2L} - i_{\pi(2l-1)}$ elements. Together with (31), we see that the $(i_{\pi(2l-1)} - i_1 + 1)$-th to $(i_{\pi(2l)} - i_1)$-th elements of $\varphi(\boldsymbol{t}_l)$ are given by $\boldsymbol{w}_l$, and the $(i_{\pi(2l)} - i_1 + 1)$-th to $(i_{2L} - i_1 + 1)$-th elements of $\varphi(\boldsymbol{t}_l)$ are given by $\boldsymbol{0}$. Then, we have

$$\boldsymbol{w}_{l,k} = \boldsymbol{0} \text{ for } k \geq \pi(2l), \tag{42}$$

and thus (40) can be represented as

$$\varphi(\boldsymbol{t}_l) = \left(\sum_{k=1}^{\pi(2l)-1} \tilde{\boldsymbol{w}}_{l,k}\right) \bmod q. \tag{43}$$

Define

$$\mathcal{K}_l = \{k | i_{\pi(2l-1)} \leq i_k \leq i_{k+1} \leq i_{\pi(2l)}\}, \quad l \in \mathcal{I}_L. \tag{44}$$

Lemma 3:

$$\tilde{\boldsymbol{w}}_l = \left(\sum_{k\in\mathcal{K}_l} \tilde{\boldsymbol{w}}_{l,k}\right) \bmod q. \tag{45}$$

Proof: From the discussion below (41), $i_{\pi(2l-1)} \leq i_k \leq i_{k+1} \leq i_{\pi(2l)}$ implies that the $(i_k - i_1 + 1)$-th to $(i_{k+1} - i_1)$-th elements of $\varphi(\boldsymbol{t}_l)$, i.e., $\boldsymbol{w}_{l,k}$, are the $(i_k - i_1 + 1)$-th to $(i_{k+1} - i_1)$-th elements of $\tilde{\boldsymbol{w}}_l$. Together (31) with the definition of $\mathcal{K}_l$ in (44), we have (45). ■

Lemma 3 implies that source message $\boldsymbol{w}_l$ only consists of the message segments $\{\boldsymbol{w}_{l,k} | k \in \mathcal{K}_l\}$, and thus we don't care the message segments $\{\boldsymbol{w}_{l,k} | 1 \leq k \leq \pi(2l-1) - 1\}$ (which are determined by $\{\boldsymbol{w}_{l,k} | k \in \mathcal{K}_l\}$).

Consider the entropy rate of $\boldsymbol{w}_{l,k}$. For $k \in \mathcal{K}_l$, $\boldsymbol{w}_{l,k}$ is uniformly distributed over $\mathbb{Z}_q^{i_{k+1}-i_k}$. Then, the normalized entropy rate of $\boldsymbol{w}_{l,k}$ is given by

$$r_{\mathrm{v},k} = \frac{i_{k+1} - i_k}{n} \log q, \quad k \in \mathcal{K}_l, \ l \in \mathcal{I}_L. \tag{46}$$

Note that the entropy of $\tilde{\boldsymbol{w}}_{l,k}$ is equal to the entropy of $\boldsymbol{w}_{l,k}$. Then, the entropy rate of $\boldsymbol{t}_l$ can be represented by

$$r_l = \sum_{k\in\mathcal{K}_l} r_{\mathrm{v},k}. \tag{47}$$

We now consider the message segments of $\boldsymbol{\theta}_l \triangleq \varphi(Q_{\Lambda_{\mathrm{s},l}}(\boldsymbol{t}_l - \beta_l \boldsymbol{d}_l))$. Denote by $\boldsymbol{\theta}_{l,k}$ the k-th message segment of $\boldsymbol{\theta}_l$. Since $Q_{\Lambda_{\mathrm{s},l}}(\boldsymbol{t}_l - \beta_l \boldsymbol{d}_l) \in \Lambda_{\mathrm{s},l} (= \Lambda_{\pi(2l-1)})$, we obtain

$$\boldsymbol{\theta}_{l,k} = \boldsymbol{0} \text{ for } k \text{ satisfying } k \geq \pi(2l-1). \tag{48}$$

Let the zero-padded $\boldsymbol{\theta}_{l,k}$ be

$$\tilde{\boldsymbol{\theta}}_{l,k} = \left[\boldsymbol{0}^{\mathrm{T}}_{i_k - i_1}, \boldsymbol{\theta}^{\mathrm{T}}_{l,k}, \boldsymbol{0}^{\mathrm{T}}_{i_{2L} - i_{k+1}}\right]^{\mathrm{T}} \in \mathbb{Z}_q^{i_{2L}-i_1}. \tag{49}$$

Then, we can rewrite $\boldsymbol{\theta}_l$ as

$$\boldsymbol{\theta}_l = \left(\sum_{k=1}^{2L} \tilde{\boldsymbol{\theta}}_{l,k}\right) \bmod q \tag{50a}$$

$$= \left(\sum_{k=1}^{\pi(2l-1)-1} \tilde{\boldsymbol{\theta}}_{l,k}\right) \bmod q, \tag{50b}$$

where (50b) follows from (48).

Based on (43) and (50), we can represent $\varphi(\tilde{\boldsymbol{t}}_l)$ in (38) as follows:

$$\varphi(\tilde{\boldsymbol{t}}_l) = \left(\sum_{k=1}^{\pi(2l)-1} \tilde{\boldsymbol{w}}_{l,k} - \sum_{k=1}^{\pi(2l-1)-1} \tilde{\boldsymbol{\theta}}_{l,k}\right) \bmod q \tag{51a}$$

$$= \left(\sum_{k\in\mathcal{K}_l} \tilde{\boldsymbol{w}}_{l,k} + \sum_{k=1}^{\pi(2l-1)-1} (\tilde{\boldsymbol{w}}_{l,k} - \tilde{\boldsymbol{\theta}})_{l,k}\right) \bmod q. \tag{51b}$$

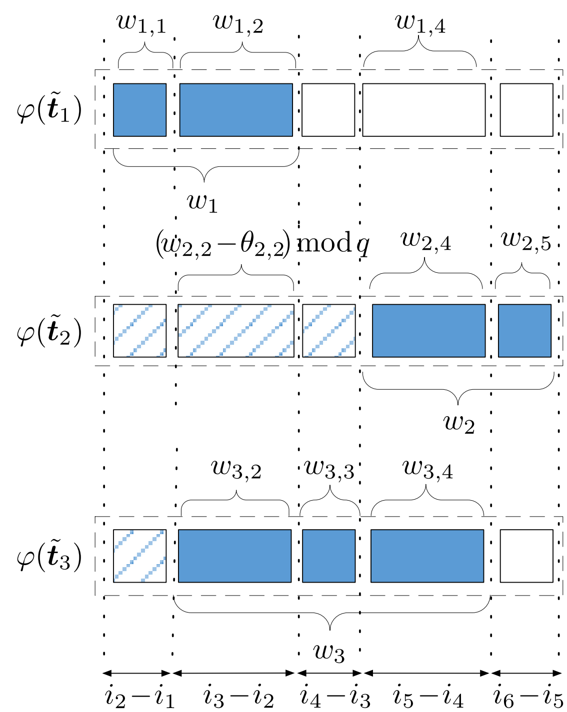

Fig. 3. An illustration of label splitting for $\{\varphi(\tilde{\boldsymbol{t}}_l)\}$ with the nested lattice chain $\Lambda_1(\Lambda_{\mathrm{s},1}) \subseteq \Lambda_2(\Lambda_{\mathrm{s},3}) \subseteq \Lambda_3(\Lambda_{\mathrm{c},1}) \subseteq \Lambda_4(\Lambda_{\mathrm{s},2}) \subseteq \Lambda_5(\Lambda_{\mathrm{c},3}) \subseteq \Lambda_6(\Lambda_{\mathrm{c},2})$. The source codewords are given by $\boldsymbol{t}_1 \in \Lambda_3 \cap \mathcal{V}_1$, $\boldsymbol{t}_2 \in \Lambda_6 \cap \mathcal{V}_4$, and $\boldsymbol{t}_3 \in \Lambda_5 \cap \mathcal{V}_2$. Each solid rectangle represents the message segment $\boldsymbol{w}_{l,k}$ satisfying $k \in \mathcal{K}_l$, i.e., being a segment of $\boldsymbol{w}_l$. For example, the message segment $\boldsymbol{w}_{1,1} \in \mathbb{Z}_q^{i_2-i_1}$ is the (i_1+1)-th to i_2-th elements of $\tilde{\boldsymbol{w}}_1$. Each blank rectangle represents the message segment being zero vectors (i.e., $\boldsymbol{w}_{l,k} = \boldsymbol{0}$).

We illustrate the label splitting of $\{\varphi(\tilde{\boldsymbol{t}}_l)\}$ in Fig. 3.

We are now ready to consider the label splitting of $\boldsymbol{u}_m \triangleq \varphi(\boldsymbol{v}_m)$. Denote by $\boldsymbol{u}_{m,k}$ the k-th message segment of $\boldsymbol{u}_m$. Let the zero-padded $\boldsymbol{u}_{m,k}$ be

$$\tilde{\boldsymbol{u}}_{m,k} = \left[\boldsymbol{0}^{\mathrm{T}}_{i_k - i_1}, \boldsymbol{u}^{\mathrm{T}}_{m,k}, \boldsymbol{0}^{\mathrm{T}}_{i_{2L} - i_{k+1}}\right]^{\mathrm{T}} \in \mathbb{Z}_q^{i_{2L}-i_1}. \tag{52}$$

Then, $\boldsymbol{u}_m$ can be represented as

$$\boldsymbol{u}_m = \bigoplus_{k=1}^{2L-1} \tilde{\boldsymbol{u}}_{m,k}. \tag{53}$$

Further, by taking the k-th message segmenmt on both side of $\varphi(\boldsymbol{v}_m) = \left(\sum_{l=1}^{L} (a_{m,l} \bmod q)\varphi(\tilde{\boldsymbol{t}}_l)\right) \bmod q$ from (37), we can rewrite $\boldsymbol{u}_{m,k}$ as

$$\boldsymbol{u}_{m,k} = \left(\sum_{l\in\mathcal{L}_k} (a_{ml} \bmod q)\boldsymbol{w}_{l,k} + \sum_{\{l|k<\pi(2l-1)\}} (a_{ml} \bmod q)(\boldsymbol{w}_{l,k} - \boldsymbol{\theta}_{l,k})\right) \bmod q \tag{54}$$

where the right hand side of (54) follows from (51) and the definition of $\mathcal{L}_k$:

$$\mathcal{L}_k = \{l | i_{\pi(2l-1)} \leq i_k \leq i_{k+1} \leq i_{\pi(2l)}\}, \quad k \in \mathcal{I}_{2L-1}. \tag{55}$$

We see that $\boldsymbol{u}_{m,k}$ can be represented as a linear combination of $\{\boldsymbol{w}_{l,k}|l \in \mathcal{L}_k\}$ plus a sum of the "don't care" message segments of $\varphi(\boldsymbol{t}_l)$ and the message segments of residual dithers. If $k \geq \pi(2l-1)$ for $l \in \mathcal{L}$, $\boldsymbol{u}_{m,k}$ can be represented as a linear combination of $\boldsymbol{w}_{l,k}$:

$$\boldsymbol{u}_{m,k} = \left(\sum_{l\in\mathcal{L}_k}(a_{ml} \bmod q)\boldsymbol{w}_{l,k}\right) \bmod q. \tag{56}$$

Lemma 4: For any given k, if $a_{ml} \neq 0$ for some $l \in \mathcal{L}_k$ (or equivalently $\boldsymbol{A}(m, \mathcal{L}_k) \neq \boldsymbol{0}$), then $\boldsymbol{u}_{m,k}$ is uniformly distributed over $\mathbb{Z}_q^{i_{k+1}-i_k}$ and independent of $\boldsymbol{u}_{m,k'}$ for any $k' > k$.

The proof of Lemma 4 is given in Appendix B.

C. Design of the Compression Function

In this subsection, we describe how to design the compression functions $\{\psi_m(\cdot)\}$ based on appropriate label splitting. With the label splitting technique in Subsection A, we show that the proposed scheme is information lossless. We refer to our approach as generalized CCF (GCCF) to distinguish it from the lattice-based CCF approach in [9].

To proceed, we map $\boldsymbol{A} \in \mathbb{R}^{L\times L}$ into $\boldsymbol{A} \bmod q \in \mathbb{Z}_q^{L\times L}$. With some abuse of notation, we replace $\boldsymbol{A} \bmod q$ simply by $\boldsymbol{A}$ in circumstances without causing ambiguity. For any $\mathcal{S} \subseteq \mathcal{I}_L, \mathcal{S}' \subseteq \mathcal{I}_L$, denote by $\boldsymbol{A}(\mathcal{S}, \mathcal{S}')$ the submatrix of $\boldsymbol{A}$ with the rows indexed by $\mathcal{S}$ and the columns indexed by $\mathcal{S}'$. Denote by $\overline{\mathcal{S}}$ the complement of $\mathcal{S}$ in $\mathcal{I}_L$. Let $\pi_\alpha(\cdot)$ be a permutation of $(1, 2, \cdots, L)$. Denote $\Pi_\alpha(\mathcal{I}_m) = \{\pi_\alpha(i)|i \in \mathcal{I}_m\}$ and $\Pi_\alpha(\emptyset) = \emptyset$. Define an index set $\mathcal{J}_m$ as

$$\mathcal{J}_m \triangleq \Big\{k|rank(\boldsymbol{A}(\Pi_\alpha(\overline{\mathcal{I}_{m-1}}), \mathcal{L}_k)) = rank(\boldsymbol{A}(\Pi_\alpha(\overline{\mathcal{I}_m}), \mathcal{L}_k)) + 1\Big\}, \tag{57}$$

where $rank(\boldsymbol{A})$ is evaluated in $\mathbb{Z}_q^{L\times L}$. From (57), we see that $k \in \mathcal{J}_m$ implies that the row $\boldsymbol{A}(\pi_\alpha(m), \mathcal{L}_k)$ is linearly independent of the rows of $\boldsymbol{A}(\pi_\alpha(\overline{\mathcal{I}_m}), \mathcal{L}_k)$. Note that $\pi_\alpha(\cdot)$ specifies an order of counting the row index of $\boldsymbol{A}$ and that $\mathcal{J}_m$ is a function of $\pi_\alpha(\cdot)$. We are now ready to present the following important result, with the proof given in Appendix C.

Theorem 1: An information lossless compression scheme is given by

$$\boldsymbol{\delta}_m = \psi(\boldsymbol{v}_m) = \bar{\psi}(\varphi(\boldsymbol{v}_m)) = \left(\sum_{k\in\mathcal{J}_{\pi_\alpha^{-1}(m)}} \tilde{\boldsymbol{u}}_{m,k}\right) \bmod q, \quad m \in \mathcal{I}_L. \tag{58}$$

We give intuitions of the compression scheme in (58). The compression aims to reduce the redundant information in $\{\boldsymbol{v}_m\}$. From (54), $\boldsymbol{u}_{m,k}$ is an integer-linear combination of $\{\boldsymbol{w}_{l,k}, l \in \mathcal{L}_k\}$ by ignoring the residual dithers $\{\boldsymbol{\theta}_{l,k}\}$ and the "don't care" message segments $\{\boldsymbol{w}_{l,k}\}$. Without dithers, we see from (57) that $\boldsymbol{u}_{\pi_\alpha(m),k}$ is linearly independent of $\{\boldsymbol{u}_{\pi_\alpha(m'),k}, m' \in \overline{\mathcal{I}_m}\}$ if $k \in \mathcal{J}_m$. Thus, the rationale of (58) is to choose the independent message segments of $\boldsymbol{v}_m$ to construct $\boldsymbol{\delta}_m$. The compression operation in (58) is illustrated in Fig. 4. A detailed example is given as follows.

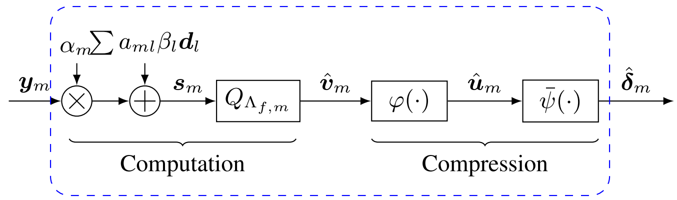

Fig. 4. Computation and compression at relay m.

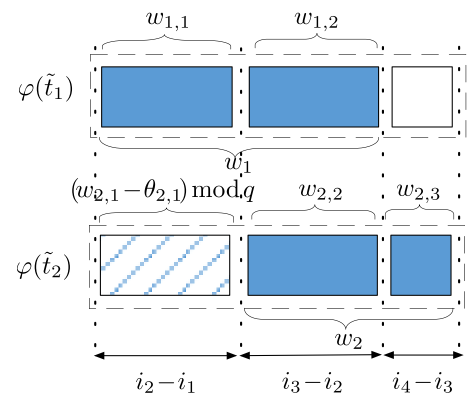

Fig. 5. Illustration of $\varphi(\tilde{\boldsymbol{t}}_1)$ and $\varphi(\tilde{\boldsymbol{t}}_2)$ in example 1.

Example 1. Consider the channel in (1) with two transmitters and two receivers. The nested lattice chain is set to $\Lambda_{s,1}(=\Lambda_1) \subseteq \Lambda_{s,2}(=\Lambda_2) \subseteq \Lambda_{c,1}(=\Lambda_3) \subseteq \Lambda_{c,2}(=\Lambda_4)$. The integer coefficient matrix is chosen as $\boldsymbol{A} = [1, 1; 1, 0]$. The computed codewords are given by

$$\boldsymbol{v}_1 = \left(\sum_{l=1}^{2} a_{1l}(\boldsymbol{t}_l - Q_{\Lambda_{s,l}}(\boldsymbol{t}_l - \beta_l\boldsymbol{d}_l))\right) \bmod \Lambda_1 \tag{59}$$

$$\boldsymbol{v}_2 = \big(a_{11}(\boldsymbol{t}_1 - Q_{\Lambda_{s,1}}(\boldsymbol{t}_1 - \beta_1\boldsymbol{d}_1))\big) \bmod \Lambda_1. \tag{60}$$

Applying the linear labeling to $\boldsymbol{v}_1$ and $\boldsymbol{v}_2$, we have

$$\boldsymbol{u}_1 = \left(\sum_{l=1}^{2} a_{1l}\varphi(\tilde{\boldsymbol{t}}_l)\right) \bmod q \tag{61}$$

$$\boldsymbol{u}_2 = \big(a_{11}\varphi(\tilde{\boldsymbol{t}}_1)\big) \bmod q. \tag{62}$$

The illustration of $\varphi(\tilde{\boldsymbol{t}}_1)$ and $\varphi(\tilde{\boldsymbol{t}}_2)$ are given in Fig. 5. By definitions in (44) and (55), we have the following index sets:

$$\mathcal{K}_1 = \{1, 2\}, \quad \mathcal{K}_2 = \{2, 3\}, \quad \mathcal{L}_1 = \{1\}, \quad \mathcal{L}_2 = \{1, 2\}, \quad \mathcal{L}_3 = \{2\}. \tag{63}$$

The prime number q is assumed to be large enough, so that the rank of $\boldsymbol{A}$ and the rank of any submatrix of $\boldsymbol{A}$ can be evaluated in the integer domain. Then, the rank functions involved in (57) are given by

$$\begin{aligned} &rank(\boldsymbol{A}(\{1\}, \mathcal{L}_1)) = 1, \quad rank(\boldsymbol{A}(\{1\}, \mathcal{L}_2)) = 1, \\ &rank(\boldsymbol{A}(\{1\}, \mathcal{L}_3)) = 1 \\ &rank(\boldsymbol{A}(\{2\}, \mathcal{L}_1)) = 1, \quad rank(\boldsymbol{A}(\{2\}, \mathcal{L}_2)) = 1, \\ &rank(\boldsymbol{A}(\{2\}, \mathcal{L}_3)) = 0 \\ &rank(\boldsymbol{A}(\mathcal{I}_2, \mathcal{L}_1)) = 1, \quad rank(\boldsymbol{A}(\mathcal{I}_2, \mathcal{L}_2)) = 2, \\ &rank(\boldsymbol{A}(\mathcal{I}_2, \mathcal{L}_3)) = 1 \\ &rank(\boldsymbol{A}(\emptyset, \mathcal{L}_1)) = 0, \quad rank(\boldsymbol{A}(\emptyset, \mathcal{L}_2)) = 0, \\ &rank(\boldsymbol{A}(\emptyset, \mathcal{L}_3)) = 0. \end{aligned} \tag{64}$$

Let $\pi_\alpha(1) = 1$ and $\pi_\alpha(2) = 2$. From (57), (63), and (64), we obtain

$$\mathcal{J}_1 = \{2, 3\} \quad \text{and } \mathcal{J}_2 = \{1, 2\}. \tag{65}$$

Then, following (58), the compression operation at receivers 1 and 2 are respectively given by

$$\begin{aligned} \boldsymbol{\delta}_1 &= \left(\tilde{\boldsymbol{u}}_{1,2} + \tilde{\boldsymbol{u}}_{1,3}\right) \bmod q \\ \boldsymbol{\delta}_2 &= \left(\tilde{\boldsymbol{u}}_{2,1} + \tilde{\boldsymbol{u}}_{2,2}\right) \bmod q. \end{aligned} \tag{66}$$

From (54) (or Fig. 5), we have

$$\boldsymbol{u}_{1,1} = \left(\boldsymbol{w}_{1,1} + (\boldsymbol{w}_{2,1} - \boldsymbol{\theta}_{2,1})\right) \bmod q \tag{67a}$$
$$\boldsymbol{u}_{1,2} = \left(\boldsymbol{w}_{1,2} + \boldsymbol{w}_{2,2}\right) \bmod q \tag{67b}$$
$$\boldsymbol{u}_{1,3} = \boldsymbol{w}_{2,3} \tag{67c}$$
$$\boldsymbol{u}_{2,1} = \boldsymbol{w}_{1,1} \tag{67d}$$
$$\boldsymbol{u}_{2,2} = \boldsymbol{w}_{1,2} \tag{67e}$$
$$\boldsymbol{u}_{2,3} = \boldsymbol{0}. \tag{67f}$$

We see that receiver 1 forwards $\boldsymbol{u}_{1,3} = \boldsymbol{w}_{2,3}$ and $\boldsymbol{u}_{1,2} = \left(\boldsymbol{w}_{1,2} + \boldsymbol{w}_{2,2}\right) \bmod q$ to the next hop, and receiver 2 forwards $\boldsymbol{u}_{2,2} = \boldsymbol{w}_{1,2}$ (independent of $\boldsymbol{u}_{1,2}$) and $\boldsymbol{u}_{2,1} = \boldsymbol{w}_{1,1}$ to the next hop. After collecting these forwarded messages, the destination can decode $\boldsymbol{w}_{2,3}$ from $\boldsymbol{u}_{1,3}$, $\{\boldsymbol{w}_{1,2}, \boldsymbol{w}_{2,2}\}$ from $\{\boldsymbol{u}_{2,2}, \boldsymbol{u}_{1,2}\}$, and $\boldsymbol{w}_{1,1}$ from $\boldsymbol{u}_{2,1}$. Thus, $\boldsymbol{w}_1$ and $\boldsymbol{w}_2$ can be successfully recovered while no redundant message is forwarded. ■

Theorem 2: The achievable compression rate tuple of (58) is given by $(R_1, R_2, \cdots, R_L)$, with R_m being the entropy rate of $\boldsymbol{\delta}_m$:

$$R_m = \frac{1}{n} H(\boldsymbol{\delta}_m) = \sum_{k \in \mathcal{J}_{\pi_\alpha^{-1}(m)}} r_{\mathrm{v},k}, \quad \text{for } m \in \mathcal{I}_L, \tag{68}$$

where $H(\cdot)$ denotes the entropy function. Further, the sum of the entropy rate of $\{\boldsymbol{\delta}_m\}$ satisfies

$$\frac{1}{n} \sum_{m=1}^{L} H(\boldsymbol{\delta}_m) = \sum_{l=1}^{L} r_l. \tag{69}$$

Eqn. (69) implies that there is no redundancy in the compressed message vectors $(\boldsymbol{\delta}_1, \boldsymbol{\delta}_2, \cdots, \boldsymbol{\delta}_L)$. The proof of Theorem 2 is given in Appendix D.

D. Relation Between GCCF and CCF

The compression function in CCF [9] is given by

$$\boldsymbol{\delta}_m = Q_{\Lambda_{d,m}}(\boldsymbol{v}_m) \bmod \Lambda_{e,m}, \quad m \in \mathcal{I}_L, \tag{70}$$

where the lattice pair $(\Lambda_{e,m}, \Lambda_{d,m})$ are chosen from the lattice chain $\Lambda_1 \subseteq \Lambda_2 \subseteq \cdots \subseteq \Lambda_{2L}$. Note that GCCF in (58) is based on the selection of message bits over $\mathbb{Z}_q^{i_{2L}-i_1}$ while CCF in (70) is based on the quantization and modulo (QM) operations over $\mathbb{R}^n$. The computation complexity of CCF is much higher than that of GCCF since QM operations over high-dimensional lattices are computationally challenging.

Moreover, redundancy may still exist after the single-QM compression in (70). For example, consider the case given by Fig. 3, where 3 transmitters communicate with 3 receivers. Suppose $\boldsymbol{A} = [2, 3, 4; 2, 1, 3; 1, 2, 3]$, and $\pi_\alpha(m) = m$ for $m \in \mathcal{I}_L$. From (57), $\mathcal{J}_2 = \{2, 4\}$. From (58), we have

$$\boldsymbol{\delta}_2 = \left(\tilde{\boldsymbol{u}}_{2,2} + \tilde{\boldsymbol{u}}_{2,4}\right) \bmod q. \tag{71}$$

In CCF, the compression function is given by

$$\boldsymbol{\delta}'_2 = Q_{\Lambda_5}(\boldsymbol{v}_2) \bmod \Lambda_2. \tag{72}$$

Note that $\boldsymbol{\delta}'_2 \in Q_{\Lambda_5} \cap \mathcal{V}_2$ and thus the rate of $\boldsymbol{\delta}'_2$ is given by $\frac{i_5 - i_2}{n} \log q$ while the rate of $\boldsymbol{\delta}_2$ is $\frac{i_5 - i_4 + i_3 - i_2}{n} \log q$. Clearly, the rate of $\boldsymbol{\delta}'_2$ is in general higher than the rate of $\boldsymbol{\delta}_2$, which implies redundancy.

In [22, Th. 1], an information lossless compression scheme based on QM operations is shown to achieve the same compression rate tuple given in Theorem 2. In the compression scheme of [22, Th. 1], multiple QM operations are applied to $\boldsymbol{v}_m$. The key technique in [22, Th. 1] is to split $\boldsymbol{v}_m$ into a set of lattice codeword components over $\mathbb{R}^n$, which is similar to the technique in Theorem 1 (i.e., splitting $\varphi(\boldsymbol{v}_m)$ into a set of message segments over $\mathbb{Z}_q^{i_{2L}-i_1}$). The computation complexity of the scheme in [22, Th. 1] is much higher than the proposed scheme in Theorem 1, due to the high complexity of QM operations.

IV. Compression Rate Region

In this section, we present an achievable compression rate region $\mathcal{R}_{\text{cpr}}$ of the proposed GCCF scheme. We also discuss the relation of the well-known Slepian-Wolf theorem and our GCCF scheme. Two examples are given to illustrate the GCCF scheme and the corresponding rate region at the end.

A. Achievable Rate Region of GCCF

We now present an achievable compression rate region $\mathcal{R}_{\text{cpr}}$ of GCCF.

Theorem 3: A compression rate region $\mathcal{R}_{\text{cpr}}$ of GCCF is given by

$$\sum_{m \in \mathcal{S}} R_m \geq f(\mathcal{S}), \quad \text{for } \mathcal{S} \subseteq \mathcal{I}_L \tag{73}$$

where

$$f(\mathcal{S}) = \sum_{k=1}^{2L-1} \left(rank(\boldsymbol{A}(\mathcal{I}_L, \mathcal{L}_k)) - rank(\boldsymbol{A}(\overline{\mathcal{S}}, \mathcal{L}_k)) \right) r_{\mathrm{v},k}. \tag{74}$$

Proof: Note that $\mathcal{R}_{\text{cpr}}$ in (73) is a polytope. Then, to prove Theorem 3, it suffices to show that GCCF can achieve all the vertices of $\mathcal{R}_{\text{cpr}}$ (by noting that the other rate tuples in $\mathcal{R}_{\text{cpr}}$ can be achieved by time sharing of vertices).

We first show how to determine the vertices of $\mathcal{R}_{\text{cpr}}$. To this end, let $\alpha_1, \cdots, \alpha_L$ be positive real numbers satisfying $\alpha_{\pi_\alpha(1)} \geq \alpha_{\pi_\alpha(2)} \geq \cdots \geq \alpha_{\pi_\alpha(L)}$. Then, a vertex of $\mathcal{R}_{\text{cpr}}$ can be found by solving the following weighted sum-rate minimization problem:

$$\text{minimize} \quad \sum_{m \in \mathcal{I}_L} \alpha_m R_m \tag{75a}$$
$$\text{subject to} \quad \sum_{m \in \mathcal{S}} R_m \geq f(\mathcal{S}), \quad \text{for } \mathcal{S} \subseteq \mathcal{I}_L. \tag{75b}$$

It can be shown that $-f(\mathcal{S})$ is a submodular function by noting the rank function is submodular and the summation preserves submodularity. From [23, pp. 70], the solution to (75) is given by $(R_1, R_2, \cdots, R_L)$ with

$$R_{\pi_\alpha(m)} = f(\Pi_\alpha(\mathcal{I}_m)) - f(\Pi_\alpha(\mathcal{I}_{m-1})), \quad \text{for } m \in \mathcal{I}_L. \quad (76)$$

That is, (76) gives the coordinates of the vertex corresponding to the permutation $\pi_\alpha(\cdot)$. By enumerating all possible $\pi_\alpha(\cdot)$, we obtain all the vertices of $\mathcal{R}_{\text{cpr}}$. What remains is to show that GCCF can achieve the rate tuple given by (76). By substituting $f(\mathcal{S})$ into (76), together with the definition of $\mathcal{J}_m$ in (57), we obtain

$$R_{\pi_\alpha(m)} = \sum_{k\in\mathcal{J}_m} r_{\text{v},k}, \quad \text{for } m \in \mathcal{I}_L. \quad (77)$$

From Theorem 2, we see that GCCF achieves the vertex of $\mathcal{R}_{\text{cpr}}$ in (76), which concludes the proof. ■

Remark 1: Since $-f(\mathcal{S})$ is a submodular function, $f(\mathcal{S})$ is a supermodular function. The rate region $\mathcal{R}_{\text{cpr}}$ given by (73) is a contra-polymatroid [24].

Remark 2: Each $\pi_\alpha(\cdot)$ determines a vertex of $\mathcal{R}_{\text{cpr}}$. However, the map between $\{\pi_\alpha(\cdot)\}$ and vertices of $\mathcal{R}_{\text{cpr}}$ is not necessarily a bijection. This implies that the total number of vertices of $\mathcal{R}_{\text{cpr}}$ may be less than $L!$.

B. Distributed Source Coding

So far, we have established the compression rate region $\mathcal{R}_{\text{cpr}}$ of GCCF. A natural question is whether the compression rate region can be further enlarged or not. From Section II-E, the compression operation is required to be information lossless, i.e., the messages $\{\boldsymbol{v}_m\}_1^L$ can be recovered from the compressed messages $\{\boldsymbol{\delta}_m\}_1^L$ without distortion. This is a distributed source coding problem [25]–[27] with the optimal compression rate region given by the Slepian-Wolf theorem [17], [28]:

$$\sum_{m\in\mathcal{S}} R_m \geq \frac{1}{n} H\left(\{\boldsymbol{v}_m | m \in \mathcal{S}\} | \{\boldsymbol{v}_m | m \in \overline{\mathcal{S}}\}\right), \quad \text{for } \mathcal{S} \subseteq \mathcal{I}_L. \quad (78)$$

We henceforth refer to the rate region in (78) as the Slepian-Wolf region $\mathcal{R}_{\text{SW}}$. Comparing (73) with (78), we see that $\mathcal{R}_{\text{cpr}} = \mathcal{R}_{\text{SW}}$ if

$$f(\mathcal{S}) = \frac{1}{n} H\left(\{\boldsymbol{v}_m | m \in \mathcal{S}\} | \{\boldsymbol{v}_m | m \in \overline{\mathcal{S}}\}\right), \quad \text{for } \mathcal{S} \subseteq \mathcal{I}_L. \quad (79)$$

The following theorem shows that (79) always holds for $\mathcal{S} = \mathcal{I}_L$.

Theorem 4: The equality in (79) always holds for $\mathcal{S} = \mathcal{I}_L$, i.e., GCCF is optimal in terms of minimizing the total compression rate.

Proof: From Theorems 2 and 3, the minimum total compression rate of GCCF is achieved at a vertex of $\mathcal{R}_{\text{cpr}}$ in (73), with the coordinates $(R_1, \cdots, R_L)$ given by (68). From (76), we obtain

$$\begin{aligned} f(\mathcal{I}_L) &= f(\mathcal{I}_L) - f(\emptyset) && (80a)\\ &= \sum_{m=1}^{L} f(\Pi_\alpha(\mathcal{I}_m)) - f(\Pi_\alpha(\mathcal{I}_{m-1})) && (80b)\\ &= \sum_{m=1}^{L} R_{\pi_\alpha(m)} && (80c)\\ &= \sum_{l=1}^{L} r_l && (80d) \end{aligned}$$

where (80d) follows from (69). For $\mathcal{S} = \mathcal{I}_L$, the right hand side (RHS) of (79) is given by

$$\begin{aligned} \frac{1}{n} H(\{\boldsymbol{v}_m | m \in \mathcal{I}_L\}) &= \frac{1}{n} H(\{\boldsymbol{t}_l | l \in \mathcal{I}_L\}) && (81a)\\ &= \sum_{l=1}^{L} r_l. && (81b) \end{aligned}$$

where (81a) follows from the fact that the map from $\{\boldsymbol{t}_l | l \in \mathcal{I}_L\}$ to $\{\boldsymbol{v}_m | m \in \mathcal{I}_L\}$ is a bijection. This concludes the proof. ■

We can further show that (79) holds in the following three situations. Note that the proofs of Theorems 5 and 6 are respectively given in Appendices E and F.

Theorem 5: Consider the interference channel in Fig. 1 with $L = 2$. The proposed GCCF scheme is optimal, i.e. $\mathcal{R}_{\text{cpr}} = \mathcal{R}_{\text{SW}}$, where $\mathcal{R}_{\text{cpr}}$ is given by (73) and $\mathcal{R}_{\text{SW}}$ is given by (78).

Theorem 6: If all the transmitters share a common shaping lattice, i.e., $\Lambda_{\text{s},1} = \cdots = \Lambda_{\text{s},L}$, then the proposed GCCF scheme achieves the Slepian-Wolf region in (78).

Remark 3: It can be shown that for $L \geq 3$, the existence of dithers in general enables a compression rate region beyond $\mathcal{R}_{\text{cpr}}$ in (73) (though the minimum total compression rate remains the same, as stated in Theorem 4). An example of $\mathcal{R}_{\text{cpr}} \neq \mathcal{R}_{\text{SW}}$ will be presented in the next subsection. It is also worth noting that to achieve a compression rate region beyond $\mathcal{R}_{\text{cpr}}$, complicated distributed source coding techniques are required. Nevertheless, this is out of the scope of the paper.

C. Examples

1) Example 2: Continue from Example 1. We now describe the compression rate region $\mathcal{R}_{\text{cpr}}$. From (47), the rate of $\boldsymbol{t}_1$ (or $\boldsymbol{w}_1$) is given by $r_1 = r_{\text{v},1} + r_{\text{v},2}$ and rate of $\boldsymbol{t}_2$ (or $\boldsymbol{w}_2$) is given by $r_2 = r_{\text{v},2} + r_{\text{v},3}$. The sum rate is given by $r_{\text{sum}} = r_{\text{v},1} + 2r_{\text{v},2} + r_{\text{v},3}$. From (64) and Theorem 3, the compression rate region is given by the following three inequalities:

$$\begin{aligned} R_1 \geq\ & (rank(\boldsymbol{A}(\mathcal{I}_2, \mathcal{L}_1)) - rank(\boldsymbol{A}(\{2\}, \mathcal{L}_1)))r_{\text{v},1}\\ & + (rank(\boldsymbol{A}(\mathcal{I}_2, \mathcal{L}_2)) - rank(\boldsymbol{A}(\{2\}, \mathcal{L}_2)))r_{\text{v},2}\\ & + (rank(\boldsymbol{A}(\mathcal{I}_2, \mathcal{L}_3)) - rank(\boldsymbol{A}(\{2\}, \mathcal{L}_3)))r_{\text{v},3}\\ =\ & r_{\text{v},2} + r_{\text{v},3} \end{aligned} \quad (82)$$

$$\begin{aligned} R_2 \geq\ & (rank(\boldsymbol{A}(\mathcal{I}_2, \mathcal{L}_1)) - rank(\boldsymbol{A}(\{1\}, \mathcal{L}_1)))r_{\text{v},1}\\ & + (rank(\boldsymbol{A}(\mathcal{I}_2, \mathcal{L}_2)) - rank(\boldsymbol{A}(\{1\}, \mathcal{L}_2)))r_{\text{v},2}\\ & + (rank(\boldsymbol{A}(\mathcal{I}_2, \mathcal{L}_3)) - rank(\boldsymbol{A}(\{1\}, \mathcal{L}_3)))r_{\text{v},3}\\ =\ & r_{\text{v},2} \end{aligned} \quad (83)$$

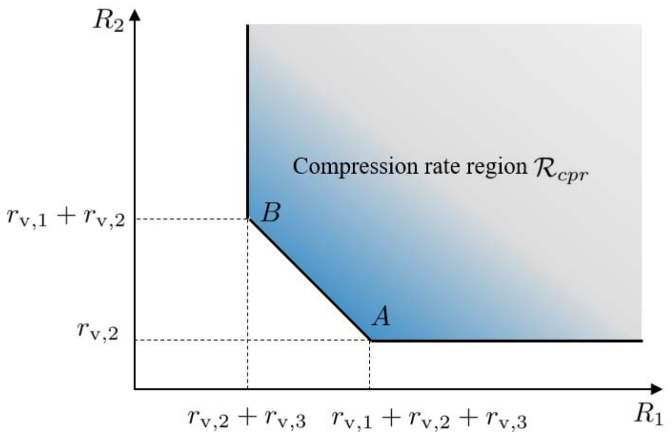

Fig. 6. The compression rate region given in (82), (83), and (84).

$$\begin{aligned} R_1+R_2 \geq\ & (rank(\boldsymbol{A}(\mathcal{I}_2,\mathcal{L}_1)) - rank(\boldsymbol{A}(\emptyset,\mathcal{L}_1)))r_{v,1} \\ & + (rank(\boldsymbol{A}(\mathcal{I}_2,\mathcal{L}_2)) - rank(\boldsymbol{A}(\emptyset,\mathcal{L}_2)))r_{v,2} \\ & + (rank(\boldsymbol{A}(\mathcal{I}_2,\mathcal{L}_3)) - rank(\boldsymbol{A}(\emptyset,\mathcal{L}_3)))r_{v,3} \\ =\ & r_{\text{sum}}. \end{aligned} \tag{84}$$

Fig. 6 illustrates the compression rate region given in (82), (83), and (84). Recall the compression operation in (66). The entropy rate of $\boldsymbol{\delta}_1$ and $\boldsymbol{\delta}_2$ are respectively given by

$$\frac{1}{n}H(\boldsymbol{\delta}_1) = r_{v,2}+r_{v,3}$$
$$\frac{1}{n}H(\boldsymbol{\delta}_2) = r_{v,1}+r_{v,2}.$$

The rate tuple $(\frac{1}{n}H(\boldsymbol{\delta}_1), \frac{1}{n}H(\boldsymbol{\delta}_2))$ corresponds to vertex B in Fig. 6, i.e., $(R_1, R_2) = (H(\boldsymbol{\delta}_1), H(\boldsymbol{\delta}_2))$.[1] Note that $\boldsymbol{v}_1 \in \Lambda_4 \cap \mathcal{V}_1$ and $\boldsymbol{v}_2 \in \Lambda_3 \cap \mathcal{V}_1$, the rate of $\boldsymbol{v}_1$ is $r_{v,1}+r_{v,2}+r_{v,3}$ and the rate of $\boldsymbol{v}_2$ is $r_{v,1}+r_{v,2}$. Therefore, by compression, the total rate is reduced from $r_{v,1}+r_{sum}$ to r_{sum}, while r_{sum} is the minimum sum rate for lossless compression.

2) Example 3: We now give an example of $\mathcal{R}_{\text{cpr}} \neq \mathcal{R}_{\text{SW}}$ for $L \geq 3$. It suffices to show that the vertex of $\mathcal{R}_{\text{cpr}}$ associated with $\pi_\alpha(\cdot)$ is not equal to the corresponding vertex of $\mathcal{R}_{\text{SW}}$. Recall that the coordinates of the vertex of $\mathcal{R}_{\text{cpr}}$ associated with $\pi_\alpha(\cdot)$ is given by (68) in Theorem 2 and the coordinates of the corresponding vertex of $\mathcal{R}_{\text{SW}}$ is given by (147) in Appendix F. Then, we need to show that there exists m and $\pi_\alpha(\cdot)$ such that

$$H(\boldsymbol{\delta}_{\pi_\alpha(m)}) \neq H\left(\boldsymbol{v}_{\pi_\alpha(m)}|\{\boldsymbol{v}_i, i \in \pi_\alpha(\overline{\mathcal{I}_m})\}\right). \tag{85}$$

Consider the nested lattice chain $\Lambda_1(\Lambda_{s,3}) \subseteq \Lambda_2(\Lambda_{s,2}) \subseteq \Lambda_3(\Lambda_{s,1}) \subseteq \Lambda_4(\Lambda_{c,3}) \subseteq \Lambda_5(\Lambda_{c,2}) \subseteq \Lambda_6(\Lambda_{c,1})$. The label $\{\varphi(\tilde{\boldsymbol{t}}_l)\}$ are illustrated in Fig. 7. Let $\pi_\alpha(m) = m$ for $m \in \mathcal{I}_L$. We assume

$$\begin{bmatrix}\boldsymbol{u}_2\\ \boldsymbol{u}_3\end{bmatrix} = \left(\begin{bmatrix}1 & 3 & 3\\ 2 & 2 & 3\end{bmatrix}\begin{bmatrix}\varphi(\tilde{\boldsymbol{t}}_1)\\ \varphi(\tilde{\boldsymbol{t}}_2)\\ \varphi(\tilde{\boldsymbol{t}}_3)\end{bmatrix}\right) \bmod q \tag{86}$$

[1]Vertex A in Fig. 6 can be achieved by the permutation $\pi_\alpha(\cdot)$ with $\pi_\alpha(1) = 2$ and $\pi_\alpha(2) = 1$.

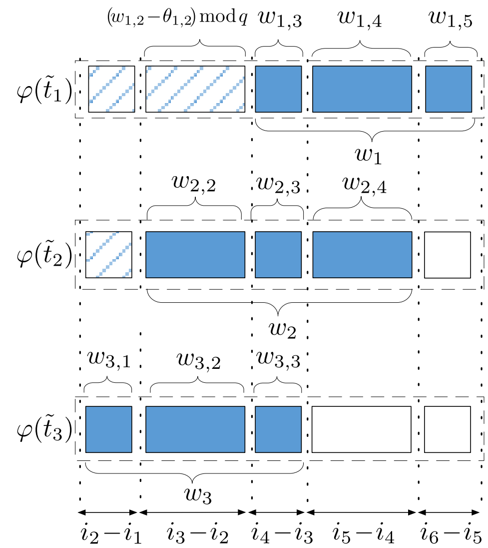

Fig. 7. The lable splitting structure for Example 3 with nested lattice chain $\Lambda_1(\Lambda_{s,3}) \subseteq \Lambda_2(\Lambda_{s,2}) \subseteq \Lambda_3(\Lambda_{s,1}) \subseteq \Lambda_4(\Lambda_{c,3}) \subseteq \Lambda_5(\Lambda_{c,2}) \subseteq \Lambda_6(\Lambda_{c,1})$.

where mod$q$ is element-wise. We now show

$$H(\boldsymbol{\delta}_2) \neq H(\boldsymbol{u}_2|\boldsymbol{u}_3). \tag{87}$$

From (58), we obtain

$$\boldsymbol{\delta}_2 = \left(\tilde{\boldsymbol{u}}_{2,2}+\tilde{\boldsymbol{u}}_{2,3}+\tilde{\boldsymbol{u}}_{2,4}\right) \bmod q. \tag{88}$$

From (68), the entropy rate of $\boldsymbol{\delta}_2$ is given by

$$H(\boldsymbol{\delta}_2) = \sum_{k=2}^{4} r_{v,k}. \tag{89}$$

By the chain rule, we have

$$\begin{aligned} H(\boldsymbol{u}_2|\boldsymbol{u}_3) =\ & H\left(\boldsymbol{u}_{2,1}|\boldsymbol{u}_3, \{\boldsymbol{u}_{2,k'}\}_{k'=2}^5\right) \\ & + H\left(\boldsymbol{u}_{2,2}|\boldsymbol{u}_3, \{\boldsymbol{u}_{2,k'}\}_{k'=3}^5\right) \\ & + H\left(\boldsymbol{u}_{2,3}|\boldsymbol{u}_3, \{\boldsymbol{u}_{2,k'}\}_{k'=4}^5\right) \\ & + H\left(\boldsymbol{u}_{2,4}|\boldsymbol{u}_3, \{\boldsymbol{u}_{2,5}\}\right) + H\left(\boldsymbol{u}_{2,5}|\boldsymbol{u}_3\right). \end{aligned} \tag{90}$$

We calculate $H\left(\boldsymbol{u}_{2,k}|\boldsymbol{u}_3, \{\boldsymbol{u}_{2,k'}\}_{k'=k+1}^5\right)$ in a descending order of k.

For $k = 5$,

$$\begin{aligned} H\left(\boldsymbol{u}_{2,5}|\boldsymbol{u}_3\right) &= H\left(\boldsymbol{u}_{2,5}|\{\boldsymbol{u}_{3,k'}\}_{k'=1}^5\right) && \text{(91a)} \\ &= H\left(\boldsymbol{u}_{2,5}|\boldsymbol{u}_{3,1}, \boldsymbol{u}_{3,2}, \boldsymbol{u}_{3,5}\right) && \text{(91b)} \end{aligned}$$

where (91b) is from the fact that $\boldsymbol{u}_{2,,5}$ and $\boldsymbol{u}_{3,k'}$ for $k' \geq 3, k' \neq 5$ can be expressed by (56) and thus $\boldsymbol{u}_{2,5}$ is independent of $\boldsymbol{u}_{3,k'}$ for $k' \geq 3, k' \neq 5$. From (56), we obtain $\boldsymbol{u}_{2,5} = \boldsymbol{w}_{1,5}$ and $\boldsymbol{u}_{3,5} = \boldsymbol{w}_{1,5}) = \boldsymbol{u}_{2,5}$. Thus,

$$H\left(\boldsymbol{v}_{2,5}|\boldsymbol{v}_{3,1}, \boldsymbol{v}_{3,2}, \boldsymbol{v}_{3,5}\right) = 0. \tag{92}$$

For $k = 4$,

$$\begin{aligned} H\left(\boldsymbol{u}_{2,4}|\boldsymbol{u}_3, \boldsymbol{u}_{2,5}\right) &= H\left(\boldsymbol{u}_{2,4}|\{\boldsymbol{u}_{3,k'}\}_{k'=1}^5, \boldsymbol{u}_{2,5}\right) && \text{(93a)} \\ &= H\left(\boldsymbol{u}_{2,4}|\boldsymbol{u}_{3,1}, \boldsymbol{u}_{3,2}, \boldsymbol{u}_{3,4}\right) && \text{(93b)} \end{aligned}$$

where (93b) follows from the fact that $\boldsymbol{u}_{2,4}$ is independent of $\boldsymbol{u}_{2,5}$ and $\boldsymbol{u}_{3,3}, \boldsymbol{u}_{3,5}$. From (54), we obtain

$$\boldsymbol{u}_{2,4} = \left(\boldsymbol{w}_{1,4} + 3\boldsymbol{w}_{2,4}\right) \bmod q, \tag{94}$$

$$\boldsymbol{u}_{3,1} = \left(2(\boldsymbol{w}_{1,1} - \boldsymbol{\theta}_{1,1}) + 2(\boldsymbol{w}_{2,1} - \boldsymbol{\theta}_{2,1}) + 3\boldsymbol{w}_{3,1}\right) \bmod q, \tag{95}$$

$$\boldsymbol{u}_{3,2} = \left(2(\boldsymbol{w}_{1,2} - \boldsymbol{\theta}_{1,2}) + 2\boldsymbol{w}_{2,2} + 3\boldsymbol{w}_{3,2}\right) \bmod \Lambda_2, \tag{96}$$

$$\boldsymbol{u}_{3,4} = \left(2\boldsymbol{t}_{1,4} + 2\boldsymbol{t}_{2,4}\right) \bmod \Lambda_4. \tag{97}$$

Since the coefficient vector $[1, 3]$ is independent of $[2, 2]$, we see from Lemma 7 that $\boldsymbol{u}_{2,4}$ is independent of $\boldsymbol{u}_{3,4}$. Folloiwng the proof of Lemma 4, we see that both $\boldsymbol{u}_{3,1}$ and $\boldsymbol{u}_{3,2}$ are independent of $\boldsymbol{w}_1$ and $\boldsymbol{w}_2$. Thus, $\boldsymbol{u}_{3,1}$ and $\boldsymbol{u}_{3,2}$ are independent of $\boldsymbol{u}_{2,4}$. Thus,

$$H\left(\boldsymbol{v}_{2,4}|\boldsymbol{v}_{3,1}, \boldsymbol{v}_{3,2}, \boldsymbol{v}_{3,4}\right) = H\left(\boldsymbol{v}_{2,4}\right) \tag{98a}$$

$$= r_{\mathrm{v},4}. \tag{98b}$$

Similarly, for $k = 3$,

$$H\left(\boldsymbol{u}_{2,3}|\boldsymbol{u}_3, \boldsymbol{u}_{2,4}, \boldsymbol{u}_{2,5}\right) = H\left(\boldsymbol{u}_{2,3}|\boldsymbol{u}_{3,3}\right) \tag{99a}$$

$$= H\left(\boldsymbol{u}_{2,3}\right) \tag{99b}$$

$$= r_{\mathrm{v},3}, \tag{99c}$$

where

$$\boldsymbol{u}_{2,3} = \left(\boldsymbol{w}_{1,3} + 3\boldsymbol{w}_{2,3} + 3\boldsymbol{w}_{3,3}\right) \bmod q \tag{100}$$

$$\boldsymbol{u}_{3,3} = \left(2\boldsymbol{w}_{1,3} + 2\boldsymbol{w}_{2,3} + 3\boldsymbol{w}_{3,3}\right) \bmod q. \tag{101}$$

For $k = 2$,

$$H\left(\boldsymbol{u}_{2,2}|\boldsymbol{u}_3, \{\boldsymbol{u}_{2,k'}\}_{k'=3}^5\right) = H\left(\boldsymbol{u}_{2,2}|\{\boldsymbol{u}_{3,k'}\}_{k'=1}^5, \{\boldsymbol{v}_{2,k'}\}_{k'=3}^5\right)$$

$$= H\left(\boldsymbol{u}_{2,2}|\boldsymbol{u}_{3,2}, \boldsymbol{u}_{3,1}, \{\boldsymbol{u}_{2,k'}, \boldsymbol{u}_{3,k'}\}_{k'=3}^5\right)$$

where

$$\boldsymbol{u}_{2,2} = \left((\boldsymbol{w}_{1,2} - \boldsymbol{\theta}_{1,2}) + 3\boldsymbol{w}_{2,2} + 3\boldsymbol{w}_{3,2}\right) \bmod q \tag{102}$$

Following the discussion below (93), $\boldsymbol{u}_{3,1}$ is independent of $\boldsymbol{w}_1$ and $\boldsymbol{w}_2$, and so is independent of $\boldsymbol{u}_{2,2}$. Also, $\boldsymbol{u}_{2,2}$ is independent of $\{\boldsymbol{u}_{2,k'}, \boldsymbol{u}_{3,k'}\}_{k'=3}^5$ for given $(\boldsymbol{w}_{1,2} - \boldsymbol{\theta}_{1,2}) \bmod q$. Thus,

$$H\left(\boldsymbol{u}_{2,2}|\boldsymbol{u}_{3,2}, \boldsymbol{u}_{3,1}, \{\boldsymbol{u}_{2,k'}, \boldsymbol{u}_{3,k'}\}_{k'=3}^5\right) \tag{103a}$$

$$= H\left(\boldsymbol{u}_{2,2}|\boldsymbol{u}_{3,2}, \{\boldsymbol{u}_{2,k'}, \boldsymbol{u}_{3,k'}\}_{k'=3}^5\right) \tag{103b}$$

$$\geq H\left(\boldsymbol{u}_{2,2}|\boldsymbol{u}_{3,2}, (\boldsymbol{w}_{1,2} - \boldsymbol{\theta}_{1,2}) \bmod q, \{\boldsymbol{u}_{2,k'}, \boldsymbol{u}_{3,k'}\}_{k'=3}^5\right) \tag{103c}$$

$$= H\left(\boldsymbol{u}_{2,2}|\boldsymbol{u}_{3,2}, (\boldsymbol{w}_{1,2} - \boldsymbol{\theta}_{1,2}) \bmod q\right) \tag{103d}$$

$$= r_{\mathrm{v},2} \tag{103e}$$

where (103e) follows from that $\boldsymbol{u}_{2,2}$ is independent of $\boldsymbol{u}_{3,2}$ for given $(\boldsymbol{w}_{1,2} - \boldsymbol{\theta}_{1,2}) \bmod q$ (by noting Lemma 7 in Appendix F), and $\boldsymbol{v}_{2,2}$ is uniformly distributed over $\mathbb{Z}_q^{i_3 - i_2}$ and independent of $(\boldsymbol{w}_{1,2} - \boldsymbol{\theta}_{1,2}) \bmod q$ (by noting Lemma 4). At the same time, we have

$$H\left(\boldsymbol{u}_{2,2}|\boldsymbol{u}_3, \{\boldsymbol{u}_{2,k'}\}_{k'=3}^5\right) \leq H\left(\boldsymbol{u}_{2,2}\right) = r_{\mathrm{v},2}. \tag{104}$$

Thus,

$$H\left(\boldsymbol{u}_{2,2}|\boldsymbol{u}_3, \{\boldsymbol{u}_{2,k'}\}_{k'=3}^5\right) = r_{\mathrm{v},2}. \tag{105}$$

For $k = 1$, we have

$$H\left(\boldsymbol{u}_{2,1}|\boldsymbol{u}_3, \{\boldsymbol{u}_{2,k'}\}_{k'=2}^5\right) \tag{106a}$$

$$= H\left(\boldsymbol{u}_{2,1}|\{\boldsymbol{u}_{3,k'}\}_{k'=1}^5, \{\boldsymbol{u}_{2,k'}\}_{k'=2}^5\right) \tag{106b}$$

$$= H\left(\boldsymbol{u}_{2,1}|\boldsymbol{u}_{3,1}, \{\boldsymbol{u}_{2,k'}, \boldsymbol{u}_{3,k'}\}_{k'=2}^5\right) \tag{106c}$$

where

$$\boldsymbol{u}_{2,1} = \left((\boldsymbol{w}_{1,1} - \boldsymbol{\theta}_{1,1}) + 3(\boldsymbol{w}_{2,1} - \boldsymbol{\theta}_{2,1}) + 3\boldsymbol{w}_{3,1}\right) \bmod q. \tag{107}$$

We next show that $\boldsymbol{u}_{2,1}$ is deterministic for given $\boldsymbol{u}_{3,1}, \{\boldsymbol{u}_{2,k'}, \boldsymbol{u}_{3,k'}\}_{k'=2}^5$, and $\boldsymbol{w}_{1,3}$. Recall that the value of $\boldsymbol{w}_{1,5}$ can be determined for given $\boldsymbol{u}_{2,5}$. Similarly, from (94) and (97), $\boldsymbol{w}_{1,4}$ and $\boldsymbol{w}_{2,4}$ can be determined for given $\boldsymbol{u}_{2,4}$ and $\boldsymbol{u}_{3,4}$. Also, from (100) and (101), $\boldsymbol{w}_{2,3}$ and $\boldsymbol{w}_{3,3}$ can be determined for given $\boldsymbol{u}_{2,3}$, $\boldsymbol{u}_{3,3}$, and $\boldsymbol{w}_{1,3}$. This further implies that $\tilde{\boldsymbol{w}}_1 = \left(\tilde{\boldsymbol{w}}_{1,3} + \tilde{\boldsymbol{w}}_{1,4} + \tilde{\boldsymbol{w}}_{1,5}\right) \bmod q$ is deterministic, and so are the "don't care" message segments $(\boldsymbol{w}_{1,1} - \boldsymbol{\theta}_{1,1}) \bmod q$ and $(\boldsymbol{w}_{1,2} - \boldsymbol{\theta}_{1,2}) \bmod q$. Consequently, from (96) and (102), $\boldsymbol{w}_{2,2}$ and $\boldsymbol{w}_{3,2}$ are deterministic by noting that $\boldsymbol{u}_{2,2}$ and $\boldsymbol{u}_{3,2}$ are given. Then, $\tilde{\boldsymbol{w}}_2 = \left(\tilde{\boldsymbol{w}}_{2,2} + \tilde{\boldsymbol{w}}_{2,3} + \tilde{\boldsymbol{w}}_{2,4}\right) \bmod q$ is deterministic, and so is the "don't care" message segment $(\boldsymbol{w}_{2,1} - \boldsymbol{\theta}_{2,1}) \bmod q$. From (95), $\boldsymbol{w}_{3,1}$ is deterministic, and so $\boldsymbol{u}_{2,1}$ in (107) is also deterministic. Thus, for given $\boldsymbol{u}_{3,1}, \{\boldsymbol{u}_{2,k'}, \boldsymbol{u}_{3,k'}\}_{k'=2}^5$, the randomness of $\boldsymbol{u}_{2,1}$ is completely determined by $\boldsymbol{w}_{1,3}$. In general, the value of $\boldsymbol{u}_{2,1}$ varies with the choice of $\boldsymbol{w}_{1,3}$. Therefore, we obtain

$$H\left(\boldsymbol{u}_{2,1}|\boldsymbol{u}_{3,1}, \{\boldsymbol{u}_{2,k'}, \boldsymbol{u}_{3,k'}\}_{k'=2}^5\right) > 0. \tag{108}$$

Combining (90), (92), (98), (99), (105), and (108), we obtain

$$H(\boldsymbol{u}_2|\boldsymbol{u}_3) > \sum_{k=2}^{4} r_{\mathrm{v},k}. \tag{109}$$

Thus, together with (89), we obtain (87). This example implies that, with random dithering, the optimal distributed source coding can achieve a rate region beyond $\mathcal{R}_{\mathrm{cpr}}$, though the minimum sum rate remains the same.

V. Performance Optimization for Multi-Hop Relay Networks

In this section, we consider a multi-hop relay network employing our GCCF relaying scheme. We first describe the GCCF scheme for a N-hop relay network and then present the achievable rates of the network. Then, we formulate the sum-rate maximization problem for a two hop relay network and present an algorithm to solve the problem. Finally, numerical results for the two hop relay network are provided for comparison.

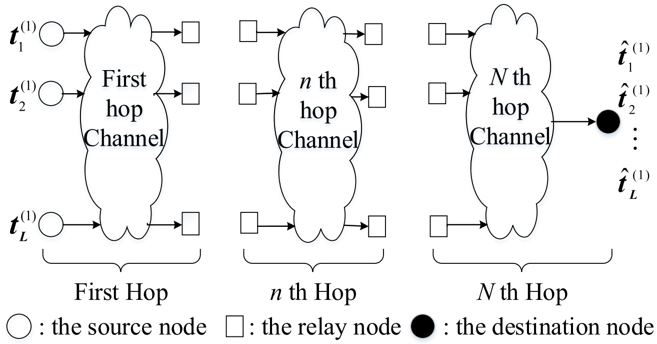

Fig. 8. A multi-hop relay network with a single destination node.

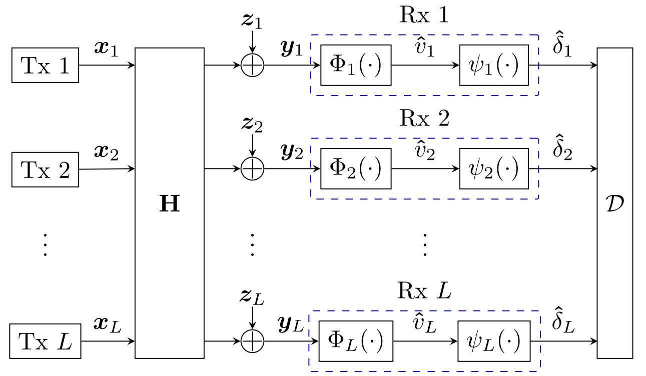

Fig. 9. A two-hop relay network with L transmitter nodes, L receiver nodes, and one destination node. Function $\Phi_l(\cdot)$ represents the decoding steps given by (24) and (25).

A. Achievable Rates

An N-hop relay network is illustrated in Fig 8. Each of the first $(N-1)$ hop is modeled by the interference channel in Fig. 1. The last hop has a unique destination node required to recover all the source messages.

We use superscript $^{(n)}$ to represent variables associated with the n-th hop. Specifically, denote by $\boldsymbol{t}_l^{(n)}$ the codeword of transmitter l in the n-th hop, and by $r_l^{(n)}$ the corresponding transmission rate. Denote by $\Lambda_1^{(n)} \subseteq \Lambda_2^{(n)} \subseteq \cdots \subseteq \Lambda_{2L}^{(n)}$ the nested lattice chain used to encode $\boldsymbol{t}_l^{(n)}$ in the n-th hop and by $r_{\mathrm{v},k}^{(n)}$ the rate of the k-th message segment in the n-th hop. Denote by $\pi^{(n)}(\cdot)$ the lattice chain permutation in the n-th hop. Denote by $\boldsymbol{A}^{(n)}$ the corresponding coefficient matrix. Note that the receivers in the n-th hop are the transmitters in the $(n+1)$-th hop. Each receiver in the n-th hop needs to re-encode the compressed message, denoted by $\boldsymbol{\delta}_m^{(n)}$, into

$$\boldsymbol{t}_m^{(n+1)} = \Psi_m^{(n)}(\boldsymbol{\delta}_m^{(n)}) \in \Lambda_{\mathrm{c},m}^{(n+1)} \cap \mathcal{V}_{\mathrm{s},m}^{(n+1)} \tag{110}$$

where $\Lambda_{\mathrm{c},m}^{(n+1)}$ is the coding lattice of m-th transmitter in $(n+1)$-th hop and $\mathcal{V}_{\mathrm{s},m}^{(n+1)}$ is the Voronoi region of the shaping lattice $\Lambda_{\mathrm{s},m}^{(n+1)}$. Denote by $r_m^{(n+1)}$ the rate of $\boldsymbol{t}_m^{(n+1)}$. The computation rate region and the compression rate region in the n-th hop are respectively denoted by $\mathcal{R}_{\mathrm{cpu}}^{(n)}$ and $\mathcal{R}_{\mathrm{cpr}}^{(n)}$, where $1 \le n \le N-1$. Denote by $\mathcal{R}^{(N)}$ the capacity region of the N-th hop. Then, an achievable transmission rate tuples of the multi-hop relay network are given in the theorem below.

Theorem 7: Consider the N-hop relay network in Fig. 8. For any given lattice chain permutations $\{\pi^n(\cdot)|n = 1,\cdots,N-1\}$, a transmission rate tuple $(r_1^{(1)}, r_2^{(1)}, \cdots, r_L^{(1)})$ is achievable when the following conditions are satisfied:

(i) $(r_1^{(n)}, r_2^{(n)}, \cdots, r_L^{(n)}) \in \mathcal{R}_{\mathrm{cpu}}^{(n)}, n \in \{1,2,\cdots,N-1\}$,
(ii) $(r_1^{(n+1)}, r_2^{(n+1)}, \cdots, r_L^{(n+1)}) \in \mathcal{R}_{\mathrm{cpr}}^{(n)}, n \in \{1,\cdots,N-1\}$,
(iii) $rank(\boldsymbol{A}^{(n)}) = L, n \in \{1,2,\cdots,N-1\}$,
(iv) $(r_1^{(n)}, r_2^{(n)}, \cdots, r_L^{(n)}) \in \mathcal{R}^{(n)}, n = N$.

Proof: Condition 7 ensures the error-free computation at the n-th hop; condition 7 ensures that the coefficient matrix is invertible and so the source messages can be recovered from the computed messages; condition 7 ensures that the computed messages can be recovered from the compressed messages. With conditions (i)-(iii), $\{\boldsymbol{t}_l^{(n)}\}_1^L$ can be recovered from $\{\boldsymbol{t}_l^{(n+1)}\}_1^L$ (or $\{\boldsymbol{\delta}_m^{(n)}\}_1^L$) successfully. Besides, condition 7 ensures the successful recovery of $\{\boldsymbol{t}_l^{(N)}\}_1^L$ at the destination node. This concludes the proof. ■

Remark 4: In Theorem 7, $(r_1^{(n)}, r_2^{(n)}, \cdots, r_L^{(n)})$ is related to $(r_1^{(n+1)}, r_2^{(n+1)}, \cdots, r_L^{(n+1)})$ as follows. From Theorem 3, for any given $\pi^n(\cdot)$, $\mathcal{R}_{\mathrm{cpr}}^{(n)}$ can be represented as a function of $\{r_{\mathrm{v},k}^{(n)}\}$. From (47), $r_l^{(n)}$ is also a function of $\{r_{\mathrm{v},k}^{(n)}\}$. Thus, condition 7 gives a constraint that relates $(r_1^{(n)}, r_2^{(n)}, \cdots, r_L^{(n)})$ to $(r_1^{(n+1)}, r_2^{(n+1)}, \cdots, r_L^{(n+1)})$.

Remark 5: The network configuration of $N = 2$ is illustrated in Fig. 9. This configuration is of particular importance due to its connection to the cloud radio access network (C-RAN) [29]. In C-RAN, baseband signal processing is carried out in a central processor (CP), rather than in base stations as in a conventional cellular network. More specifically, in an uplink C-RAN, the function of a base station is reduced to receive radio signals from mobile users and then forward the signal to the CP after simple processing, while the CP collects signals from all the base stations and jointly decodes the messages of mobile users. Zhou and Yu [30] and Park *et al.* [31] proposed to quantize the received signal at base stations and forward the quantized signal to the CP. It was shown that with optimized quantization, C-RAN achieves a much higher sum rate than a conventional cellular network does. Interestingly, C-RAN can be modelled by the two-hop relay network described in Fig. 9, where the receivers serve as the base stations in C-RAN, and the single destination node serves as the CP. With this analogy, the achievable rate region developed in Theorem 7 can be used to characterize the performance limits for the uplink C-RAN.

B. Sum-Rate Maximization

In this subsection, we consider the sum-rate maximization of the network in Fig. 8. We focus on the case of $N = 2$ illustrated in Fig. 9. Based on Theorem 7 and some other encoding constraints, we can formulate the sum-rate maximization problem as

$$\underset{\mathcal{O}}{\text{maximize}} \quad \sum_{l=1}^{L} r_l^{(1)} \tag{111a}$$

$$\text{subject to} \quad p_l \le P_l, \quad \beta_l > 0, \tag{111b}$$

$$\pi(2l-1) < \pi(2l), \tag{111c}$$
$$r_l^{(1)} = \sum_{k\in\mathcal{K}_l} r_{\mathrm{v},k}^{(1)}, \quad \text{for } l \in \mathcal{I}_L, \tag{111d}$$
$$\sum_{k\in\mathcal{P}_l} r_{\mathrm{v},k}^{(1)} = \frac{1}{2}\log\frac{\left(\beta_{\pi_s(l)}^{(1)}\right)^2 p_{\pi_s(l)}^{(1)}}{\left(\beta_{\pi_s(l+1)}^{(1)}\right)^2 p_{\pi_s(l+1)}^{(1)}}, \quad \text{for } l\in\mathcal{I}_{L-1}, \tag{111e}$$
$$r_{\mathrm{v},k}^{(1)} \geq 0, \quad \text{for } k \in \mathcal{I}_{2L-1}, \tag{111f}$$
$$(r_1^{(1)}, r_2^{(1)}, \cdots, r_L^{(1)}) \in \mathcal{R}_{\mathrm{cpu}}^{(1)}, \tag{111g}$$
$$(r_1^{(2)}, r_2^{(2)}, \cdots, r_L^{(2)}) \in \mathcal{R}_{\mathrm{cpr}}^{(1)}, \tag{111h}$$
$$(r_1^{(2)}, r_2^{(2)}, \cdots, r_L^{(2)}) \in \mathcal{R}^{(2)}, \tag{111i}$$
$$rank(\boldsymbol{A}^{(1)}) = L, \tag{111j}$$

where $\mathcal{O} = \left\{\{\beta_l^{(1)}\}_1^L, \{p_l^{(1)}\}_1^L, \{r_{\mathrm{v},k}^{(1)}\}_1^{2L-1}, \{r_m^{(2)}\}_1^L, \pi(\cdot)^{(1)}, \boldsymbol{A}^{(1)}\right\}$, and $\mathcal{P}_l = \{k | i_{\pi(2\pi_s(l)-1)}^{(1)} \leq i_k^{(1)} < i_{k+1}^{(1)} \leq i_{\pi(2\pi_s(l+1)-1)}^{(1)}\}$.

In the above formulation, (111c) is from (15); (111d) is from (47); (111g)-(111j) are from Theorem 7. Eqn. (111e) establishes the relations between the rates of the message segments and the source powers $\{p_l^{(1)}\}$. More specifically, consider a message $\boldsymbol{w}$ uniformly distributed over the finite field $\mathbb{Z}_q^{i_{\pi(2\pi_s(l+1)-1)}^{(1)} - i_{\pi(2\pi_s(l)-1)}^{(1)}}$. The entropy rate of the message $\boldsymbol{w}$ is equal to the rate of a nested lattice code with codebook $\Lambda_{s,\pi_s(l+1)}^{(1)} \cap \mathcal{V}_{s,\pi_s(l)}^{(1)}$. From (18) and (22), the entropy rate is given by $\frac{1}{2}\log\frac{\left(\beta_{\pi_s(l)}^{(1)}\right)^2 p_{\pi_s(l)}^{(1)}}{\left(\beta_{\pi_s(l+1)}^{(1)}\right)^2 p_{\pi_s(l+1)}^{(1)}}$. Note that $\boldsymbol{w} \in \mathbb{Z}_q^{i_{\pi(2\pi_s(l+1)-1)}^{(1)} - i_{\pi(2\pi_s(l)-1)}^{(1)}}$ can be split into a set of message segments indexed given by $\mathcal{P}_l$. Therefore, the rate of $\boldsymbol{w}$ can be represented by the LHS of (111e).

C. Approximate Solution

The maximization problem in (111) is an NP-hard mixed integer programming problem. We now present an approximate algorithm to solve (111). For any given $\{\beta_l^{(1)}\}, \{p_l^{(1)}\}$, and $\pi(\cdot)^{(1)}$ satisfying (111c) and (111b), we can solve (111) by the following steps:

- Following [9], find a suboptimal coefficient matrix $\boldsymbol{A}$ by using the LLL algorithm in [15];
- Determine $\mathcal{R}_{\mathrm{cpu}}^{(1)}$ by (27) and $\mathcal{R}_{\mathrm{cpr}}^{(1)}$ by (73);
- Optimize $\{r_{\mathrm{v},k}^{(1)}\}$ and $\{r_{\mathrm{m}}^{(2)}\}$ using linear programming.

The above procedures are summarized in Algorithm 1. What remains is to optimize $\pi(\cdot)^{(1)}, \{\beta_l^{(1)}\}$, and $\{p_l^{(1)}\}$. Here we employ the brute-force method to optimize $\pi(\cdot)^{(1)}$ and the differential evolution algorithm [18] to optimize $\{\beta_l^{(1)}\}$ and $\{p_l^{(1)}\}$.

The exhaustive search over $\pi(\cdot)^{(1)}$ needs to consider $(2L)!$ different permutations, and is time-consuming even for a moderate L. In what follows, we describe a method to reduce the complexity when the separability condition in (114) is satisfied. With (114), the nested lattice chain can be represented by $\Lambda_{s,\pi_s(1)}^{(1)} \subseteq \Lambda_{s,\pi_s(2)}^{(1)} \subseteq \cdots \subseteq \Lambda_{s,\pi_s(L)}^{(1)} \subseteq \Lambda_{c,\pi_c(1)}^{(1)} \subseteq \Lambda_{c,\pi_c(2)}^{(1)} \subseteq \cdots \subseteq \Lambda_{c,\pi_c(L)}^{(1)}$. From (22), the permutation $\pi_s(\cdot)$ satisfies the inequality:

$$(\beta_{\pi_s(1)}^{(1)})^2 p_{\pi_s(1)}^{(1)} \geq \cdots \geq (\beta_{\pi_s(L)}^{(1)})^2 p_{\pi_s(L)}^{(1)}. \tag{112}$$

For given $\{\beta_l^{(1)}\}_{l=1}^L$ and $\{p_l^{(1)}\}_{l=1}^L$, $\pi_s(\cdot)^{(1)}$ is uniquely determined by (112). Thus, the search space of $\pi(\cdot)^{(1)}$ reduces to the set of all possible $\pi_c(\cdot)^{(1)}$ with complexity $L!$. In general, imposing the separability condition may incur a certain performance loss by reducing the search space. However, we will see from numerical results that such a performance loss is usually marginal.

Algorithm 1 Approximate Algorithm

Require: $\boldsymbol{H}^{(1)}, \boldsymbol{H}^{(2)}, \pi(\cdot)^{(1)}, \{\beta_l^{(1)}\}_{l=1}^L, \{p_l^{(1)}\}_{l=1}^L, \{p_l^{(2)}\}_{m=1}^M$.
Ensure: $\sum_{l=1}^L r_l^{(1)}$.
1: Reorder $\{\beta_l^{(1)}\}_{l=1}^L, \{p_l^{(1)}\}_{l=1}^L$ to satisfy (112).
2: Apply LLL algorithm [15] to find a full rank $\boldsymbol{A}$.
3: With $\{p_l^{(1)}\}_{l=1}^L, \{\beta_l^{(1)}\}_{l=1}^L, \boldsymbol{H}^{(1)}$, and $\boldsymbol{A}^{(1)}$, compute $\mathcal{R}_{\mathrm{cpu}}^{(1)}$ in (27) and (28).
4: With $\boldsymbol{A}^{(1)}$ and $\pi(\cdot)^{(1)}$, compute $\mathcal{R}_{\mathrm{cpr}}^{(1)}$ in (73).
5: With $\boldsymbol{H}^{(2)}$ and $\{p_l^{(2)}\}_{m=1}^M$, compute $\mathcal{R}^{(2)}$.
6: Solve (111) by linear programming.

D. Numerical Results

In simulation, we assume that the second hop channel of Fig. 9 is a parallel channel. That is, the destination observes $\boldsymbol{y}_m' = h_m \boldsymbol{x}_m' + \boldsymbol{z}_m'$ from relay m, where h_m is the channel gain, $\boldsymbol{x}_m' \in \mathbb{R}^{n\times 1}$ is the signal forwarded by relay m with power $p_m^{(2)} = \frac{1}{n}\|\boldsymbol{x}_m'\|^2$, and z_m' is independently drawn from $\mathcal{N}(0,1)$. Therefore, the capacity region of the second hop is given by

$$\mathcal{R}^{(2)} = \left\{(r_1^{(2)}, r_2^{(2)}, \cdots, r_L^{(2)}) | r_m^{(2)} < \frac{1}{2}\log(1 + h_m^2\ p_m^{(2)}), m \in \mathcal{I}_L\right\}.$$

In our simulation, we use the toolbox Scipy [32] to realize the differential evolution and the linear programming algorithm. We average the numerical results over 1000 channel realizations. The following settings are employed: $P_l = P, 0.1 \leq \beta_l \leq 4, l \in \mathcal{I}_L$, and $p_m^{(2)} = 0.25P, m \in \mathcal{I}_L$.

1) Comparison of Various Relaying Schemes: We compare the following five relaying schemes and the cut-set upper bound in a 3×3 network:

- AF: amplify-and-forward
- DF: decode-and-forward
- CF: the asymmetric CF scheme [3]
- CCF: the original CCF scheme [9]
- GCCF: generalized compute-compress-and-forward
- Cut-set bound: a cut-set upper bound given by

$$\min\left\{\frac{1}{2}\log\det(\boldsymbol{I} + \mathrm{SNR}\boldsymbol{H}^{(1)}\boldsymbol{H}^{(1)\mathrm{T}}),\right.$$
$$\left.\sum_{m=1}^{L}\frac{1}{2}\log(1 + h_m^2 p_m^{(2)})\right\} \tag{113}$$

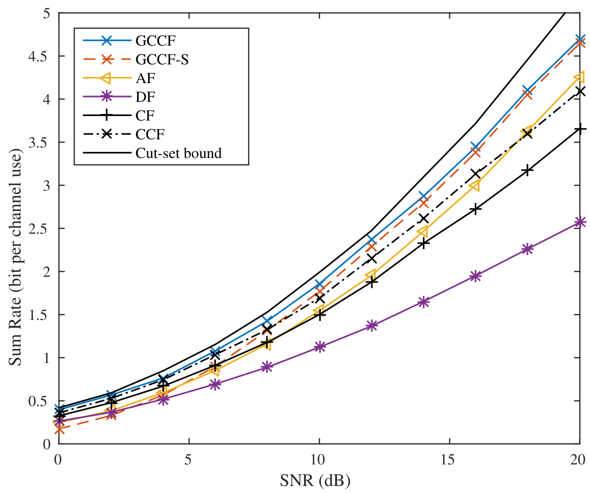

Fig. 10. The performance comparison of various relaying schemes in the two-hop relay network in Fig. 9.

- GCCF-S: generalized compute-compress-and-forward under the *separability condition* [2]

$$\Lambda_{\mathrm{s},l} \subseteq \Lambda'_{\mathrm{c},l}, \quad \text{for } l, l' \in \mathcal{I}_L. \tag{114}$$

The numerical results are presented in Fig. 10. We see that the GCCF scheme performs better than the other relaying schemes, especially at relatively high SNR. GCCF-S performs close to GCCF in the high SNR regime (SNR $>$ 10dB). This implies that GCCF-S is an attractive low-complexity alternative to GCCF in the high SNR regime.

It is interesting to compare the complexity and overhead of CF, CCF, and GCCF. Compared with CF and CCF, the only difference of GCCF is in the compression operation. CF does not perform compression, and thus does not require any extra complexity or overhead. As for CCF and GCCF, the compression of GCCF is more general and can achieve a broader rate region. The complexity of GCCF can be lower than that of CCF since the compression of GCCF is operated over finite fields (which generally requries much lower complexity than the QM operations over lattices). In terms of extra overhead for compression, both CCF and GCCF need to inform each relay how to conduct compression. Thus, the extra overheads for compression are comparable.

2) Comparison in Various Network Sizes: The numerical results for the considered relay network with sizes 2×2 and 4×4 are presented in Fig. 11. Note that the performance of GCCF is replaced by its low-complexity alternative GCCF-S. From Fig. 11, we see that GCCF-S achieves a much higher sum rate than CCF and CF does. More importantly, the rate slop of GCCF-S is higher than that of CF. The gap between GCCF-S and the cut-set bound is only 1 bit per channel use in the 4×4 network with SNR $= 20$ dB, and the gap reduces as the decrease of SNR.

[2]Intuitively, the separability condition says that, in the nested lattice chain, the finest shaping lattice is coarser than the coarsest coding lattice. With the constraint, we can decrease the complexity in optimization.

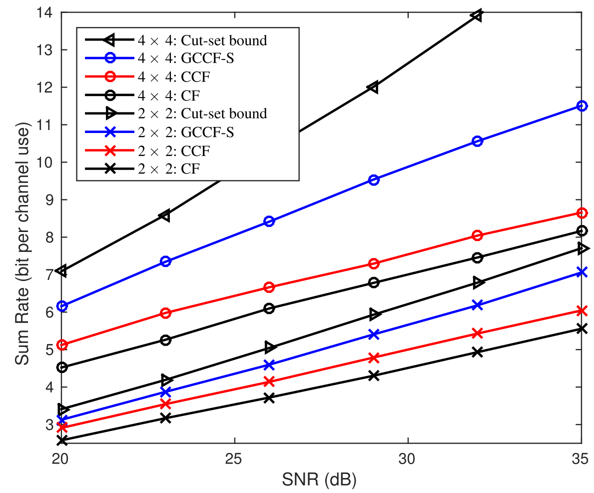

Fig. 11. The performance comparison of various schemes in the two-hop relay network in Fig. 9 with different network sizes.

VI. Conclusion

In this paper, we developed a general compression framework, termed GCCF, for CF-based relay networks. In contrast to the QM operation in the original CCF, our proposed GCCF scheme allows each relay to select message segments over finite fields, so as to reduce the information redundancy as well as the computational complexity. We showed that the compression rate region of GCCF is a contra-polymatroid and is broader than that of CCF. We also showed that GCCF is optimal in the sense of minimizing the total compression rate, and established sufficient conditions for GCCF to achieve the optimal SW region. Based on that, we studied the sum-rate maximization of the GCCF-based two-hop relay network, and demonstrated the superior performance of GCCF over the other relaying schemes.

With GCCF, there are a number of future research directions worth pursuing. First, recall that a connection between the two-hop relay network and C-RAN was established in Section V-A. This inspires us to utilize the analytical results in this paper to characterize the fundamental performance limits of C-RAN. Some initial results on the incorporation of CF techniques into C-RAN can be found, e.g., in [12]. Second, the GCCF scheme can be potentially combined with other relaying strategies, such as decode-and-forward and amplify-and-forward, to enhance the network performance. How to analyze and optimize these hybrid-relaying schemes is an interesting research topic. Third, the GCCF scheme considered in this paper assumes single-antenna transmitters and single-antenna receivers. It is known that multi-antenna techniques can be employed to dramatically increase the system capacity. As such, how to extend the results in this paper to multi-antenna relay networks is an interesting topic worth of future research effort.

Appendix A
Proof of Lemma 2

To show that $\varphi(\cdot)$ is a bijection between $\Lambda_{2L} \cap \mathcal{V}_1$ and $\mathbb{Z}_q^{i_{2L}-i_1}$, it suffices to show

$$|\Lambda_{2L} \cap \mathcal{V}_1| = |\mathbb{Z}_q^{i_{2L}-i_1}|, \tag{115}$$

and for $\boldsymbol{t}_1, \boldsymbol{t}_2 \in \Lambda_{2L} \cap \mathcal{V}_1$

$$\varphi(\boldsymbol{t}_1) = \varphi(\boldsymbol{t}_2) \quad \text{if and only if } \boldsymbol{t}_1 = \boldsymbol{t}_2. \tag{116}$$

We first show (115). Recall that the mapping in (17) is an isomorphism between $\mathbb{Z}_q^{b_l}$ and $\mathcal{C}_l$. By letting $\pi(2l-1) = 1$ and $\pi(2l) = 2L$, we obtain $b_l = i_{2L} - i_1$ and $|\Lambda_{2L} \cap \mathcal{V}_1| = |\mathbb{Z}_q^{i_{2L}-i_1}|$.

We then show (116). If $\boldsymbol{t}_1 = \boldsymbol{t}_2$, it is clear that $\varphi(\boldsymbol{t}_1) = \varphi(\boldsymbol{t}_2)$. What remains is to show the only if part. From (34), for $\boldsymbol{t}_1, \boldsymbol{t}_2 \in \Lambda_{2L} \cap \mathcal{V}_1$, we have

$$\boldsymbol{t}_1 = \bar{\varphi}(\tilde{\boldsymbol{w}}_1) \bmod \Lambda_1 \tag{117}$$
$$\boldsymbol{t}_2 = \bar{\varphi}(\tilde{\boldsymbol{w}}_2) \bmod \Lambda_1. \tag{118}$$

Further, by taking linear labeling on the both sides of (117), we have

$$\begin{aligned} \varphi(\boldsymbol{t}_1) &= \varphi\left(\bar{\varphi}(\tilde{\boldsymbol{w}}_1) - Q_{\Lambda_1}\left(\bar{\varphi}(\tilde{\boldsymbol{w}}_1)\right)\right) && \text{(119a)}\\ &= (\tilde{\boldsymbol{w}}_1 - \boldsymbol{0}) \bmod q && \text{(119b)}\\ &= \tilde{\boldsymbol{w}}_1 && \text{(119c)} \end{aligned}$$

where in (119b) $\varphi\left(\bar{\varphi}(\tilde{\boldsymbol{w}}_1)\right) = \tilde{\boldsymbol{w}}_1$ is from (32) and $\varphi\left(Q_{\Lambda_1}\left(\bar{\varphi}(\tilde{\boldsymbol{w}}_1)\right)\right) = \boldsymbol{0}$ is from the fact of $Q_{\Lambda_1}\left(\bar{\varphi}(\tilde{\boldsymbol{w}}_1)\right) \in \Lambda_1$. Similarly, we have $\varphi(\boldsymbol{t}_2) = \tilde{\boldsymbol{w}}_2$. Thus, if $\varphi(\boldsymbol{t}_1) = \varphi(\boldsymbol{t}_2)$, i.e., $\tilde{\boldsymbol{w}}_1 = \tilde{\boldsymbol{w}}_2$, we obtain $\boldsymbol{t}_1 = \boldsymbol{t}_2$ from (34). This concludes the proof.

APPENDIX B
PROOF OF LEMMA 4

We first show that $\boldsymbol{u}_{m,k}$ is uniformly distributed over $\mathbb{Z}_q^{i_{k+1}-i_k}$. Represent $\boldsymbol{u}_{m,k}$ in (54) as

$$\boldsymbol{u}_{m,k} = \left(\boldsymbol{w}_k + \boldsymbol{w}'_k\right) \bmod q \tag{120}$$

where $\boldsymbol{w}_k = \left(\sum_{l \in \mathcal{L}_k} (a_{ml} \bmod q)\boldsymbol{w}_{l,k}\right) \bmod q$ and $\boldsymbol{w}'_k = \left(\sum_{\{l | k < \pi(2l-1)\}} (a_{ml} \bmod q)(\boldsymbol{w}_{l,k} - \boldsymbol{\theta}_{l,k})\right) \bmod q$. Since there exists non-zero coefficient a_{ml} for $l \in \mathcal{L}_k$, $\boldsymbol{w}_k$ is uniformly distributed over $\mathbb{Z}_q^{i_{k+1}-i_k}$ (by noting that $\{\boldsymbol{w}_{l,k} | l \in \mathcal{L}_k\}$ are all uniformly distributed over $\mathbb{Z}_q^{i_{k+1}-i_k}$). For any given $\boldsymbol{w}'_k$, $\boldsymbol{u}_{m,k}$ is uniformly distributed over $\mathbb{Z}_q^{i_{k+1}-i_k}$. Thus, $\boldsymbol{u}_{m,k}$ is uniformly distributed over $\mathbb{Z}_q^{i_{k+1}-i_k}$ and is independent of $\boldsymbol{w}'_k$.

We now show that $\boldsymbol{u}_{m,k}$ is independent of $\boldsymbol{u}_{m,k'}$ for any $k' > k$. Since $\boldsymbol{w}_{l,k}$ is independent of $\boldsymbol{w}_{l,k'}$ for $k, k' \in \mathcal{K}_l$, then $\boldsymbol{w}_k$ in (120) is independent of $\boldsymbol{w}_{k'}$. Since $\boldsymbol{w}'_{k'}$ in $\boldsymbol{u}_{m,k'}$ is also independent of $\boldsymbol{w}_k$, together with the fact that $\boldsymbol{u}_{m,k}$ is independent of $\boldsymbol{w}'_k$, we see that $\boldsymbol{u}_{m,k}$ is independent of $\boldsymbol{u}_{m,k'}$. This concludes the proof.

APPENDIX C
PROOF OF THEOREM 1

Since $\boldsymbol{A}$ is invertible, there is a bijection between $\{\boldsymbol{v}_m\}_1^L$ and $\{\boldsymbol{t}_l\}_1^L$. Thus, to prove that $\{\boldsymbol{v}_m\}_1^L$ can be recovered from $\{\boldsymbol{\delta}_m\}_1^L$, it suffices to show that $\{\boldsymbol{w}_l\}_1^L$ can be recovered from $\{\boldsymbol{\delta}_m\}_1^L$. From (45), for any given l, $\boldsymbol{w}_l$ can be recovered from $\{\boldsymbol{w}_{l,k} | k \in \mathcal{K}_l\}$. Thus, we only need to show that $\{\boldsymbol{w}_{l,k} | l \in \mathcal{I}_L, k \in \mathcal{K}_l\}$ can be recovered from $\{\boldsymbol{\delta}_m\}_1^L$, or equivalently, $\{\boldsymbol{w}_{l,k} | l \in \mathcal{L}_k\}$ for each $k \in \mathcal{I}_{2L-1}$ can be recovered from $\{\boldsymbol{\delta}_m\}_1^L$. In the following, we show that $\{\boldsymbol{w}_{l,k} | l \in \mathcal{L}_k\}$ can be recovered recursively in a descending order of k.

To start with, we establish a relation between $\{\boldsymbol{\delta}_m\}$ and $\{\boldsymbol{u}_{m,k}\}$ as follows. From (58) in Theorem 1, we see that $\boldsymbol{\delta}_m$ contains $\boldsymbol{u}_{m,k}$ for $k \in \mathcal{J}_{\pi_\alpha^{-1}(m)}$. For any given k, define

$$\mathcal{M}_k = \left\{\text{all } m \text{ satisfying } k \in \mathcal{J}_{\pi_\alpha^{-1}(m)}\right\}. \tag{121}$$

Following the label splitting in Section III-A, we define $\boldsymbol{\delta}_{m,k}$ to be the (i_k+1)-th to (i_{k+1})-th elements of $\boldsymbol{\delta}_m$. For any $m \in \mathcal{M}_k$, we have

$$\boldsymbol{\delta}_{m,k} = \boldsymbol{u}_{m,k}. \tag{122}$$

If $m \notin \mathcal{M}_k$, we have $\boldsymbol{\delta}_{m,k} = \boldsymbol{0}$.

We first consider the recovery of $\{\boldsymbol{w}_{l,k} | l \in \mathcal{L}_k\}$ for k satisfying $i_k \geq i_{\pi(2l-1)}, l \in \mathcal{L}$ (i.e., $\boldsymbol{u}_{m,k}$ can be represented as (56)). Without loss of generality, we henceforth assume $\Lambda_{s,L} \subseteq \Lambda_{s,L-1} \subseteq \cdots \subseteq \Lambda_{s,1}$. Note that $\Lambda_{s,l} = \Lambda_{\pi(2l-1)}$ in (16). We see that the largest $i_{\pi(2l-1)}$ is $i_{\pi(1)}$. Therefore, the range of k considered in this step is given by $\pi(1) \leq k \leq 2L-1$.[3]

Thus, for any k satisfying $\pi(1) \leq k \leq 2L-1$ and $m \in \mathcal{M}_k$, $\boldsymbol{\delta}_{m,k}$ can be represented as

$$\begin{aligned} \boldsymbol{\delta}_{m,k} &= \boldsymbol{u}_{m,k} && \text{(123a)}\\ &= \left(\sum_{l \in \mathcal{L}_k} a_{ml}\boldsymbol{w}_{l,k}\right) \bmod q && \text{(123b)} \end{aligned}$$

where (123a) is from (122), and (123b) follows from the (56).

By taking transpose on the both sides of (123) and then stacking row by row for $m \in \mathcal{M}_k$, we obtain

$$\boldsymbol{\Delta}_k = \boldsymbol{A}(\mathcal{M}_k, \mathcal{L}_k)\boldsymbol{W}_k \tag{124}$$

where the i-th rows of $\boldsymbol{\Delta}_k$ is given by the transpose of $\boldsymbol{\delta}_{m_i,k}$ with m_i being the i-th element of $\mathcal{M}_k$ (ordered in an ascending manner), and the i-th row of $\boldsymbol{W}_k$ is given by the transpose of $\boldsymbol{w}_{l_i,k}$ with l_i being the i-th element of $\mathcal{L}_k$ (ordered in an ascending manner). The following lemma states that $\boldsymbol{A}(\mathcal{M}_{\pi_\alpha}^k, \mathcal{L}_k)$ is invertible.

Lemma 5: The two sets defined in (55) and (121) have the same cardinality, i.e., $|\mathcal{L}_k| = |\mathcal{M}_k|$. Further, the submatrix $\boldsymbol{A}(\mathcal{M}_k, \mathcal{L}_k)$ is invertible over $\mathbb{Z}_q^{|\mathcal{L}_k| \times |\mathcal{L}_k|}$.

Proof: From the definition of $\mathcal{M}_k$ in (121), we can construct $\mathcal{M}_k$ as follows. For each m, we consider the $\pi_\alpha(m)$-th row of the submatrix $\boldsymbol{A}(:, \mathcal{L}_k)$. If the $\pi_\alpha(m)$-th row is independent of the $\pi_\alpha(m+1)$-th, $\cdots$, $\pi_\alpha(L)$-th rows of $\boldsymbol{A}(:, \mathcal{L}_k)$, we have $m \in \mathcal{M}_k$. As $\boldsymbol{A}$ is invertible, the columns of $\boldsymbol{A}$ are independent. Thus, rank$(\boldsymbol{A}(:, \mathcal{L}_k)) = |\mathcal{L}_k|$, and so there are $|\mathcal{L}_k|$ independent rows in $\boldsymbol{A}(:, \mathcal{L}_k)$. Thus, $|\mathcal{M}_k| = |\mathcal{L}_k|$. Also, as the $|\mathcal{M}_k|$ selected rows are linearly independent, we obtain that $\boldsymbol{A}(\mathcal{M}_k, \mathcal{L}_k)$ is invertible. ∎

From Lemma 5, we recover $\boldsymbol{W}_k$ by

$$\boldsymbol{W}_k = \left(\boldsymbol{A}(\mathcal{M}_k, \mathcal{L}_k)\right)^{-1} \boldsymbol{\Delta}_k, \tag{125}$$

[3]For the example in Fig. 7, the finest shaping lattice is Λ_3. Thus, we have $\pi(1) = 3$, and so the considered range of k is $3 \leq k \leq 5$. Clearly, $\boldsymbol{u}_{m,k}$ is solely a linear combination of $\{\boldsymbol{w}_{l,k} | l \in \mathcal{L}_k\}$ for $k = 3, 4$, and 5.

which implies that $\{\boldsymbol{w}_{l,k}|l \in \mathcal{L}_k\}$ can be recovered for $\pi(1) \leq k \leq 2L-1$. Recall from (16) that $\Lambda_{c,l} = \Lambda_{\pi(2l)}$ for $l \in \mathcal{I}_L$. Thus, from (44), we obtain $\mathcal{K}_1 = \{k|\pi(1) \leq k \leq \pi(2)\} \subseteq \{k|\pi(1) \leq k \leq 2L-1\}$. Therefore, $\{\boldsymbol{w}_{1,k}|k \in \mathcal{K}_1\}$ are all recoverable and so $\boldsymbol{w}_1$ can be recovered by using (45).

We now consider the recovery of $\{\boldsymbol{w}_{l,k}\}$ for $1 \leq k \leq \pi(1)-1$ (i.e., the range of k such that $\boldsymbol{u}_{m,k}$ given by (54)). We first show the recovery of $\{\boldsymbol{w}_{l,k}\}$ for $k = \pi(1)-1$.[4] From $\Lambda_{s,2} \subseteq \Lambda_{s,1} = \Lambda_{\pi(1)}$ and the fact that Λ_k is the finest lattice which is coarser than $\Lambda_{\pi(1)}$, we have

$$i_{\pi(2*2-1)} \leq i_k < i_{\pi(2*1-1)}. \tag{126}$$

Then, from (54), $\boldsymbol{\delta}_{m,k}$ is given by

$$\boldsymbol{\delta}_{m,k} = \left(\sum_{l\in\mathcal{L}_k} a_{ml}\boldsymbol{w}_{l,k} + a_{m1}(\boldsymbol{\theta}_{1,k} - \boldsymbol{w}_{1,k})\right) \bmod q. \tag{127}$$

Note that $\boldsymbol{w}_{1,k}$ and $\boldsymbol{\theta}_{1,k}$ (the label segment of $Q_{\Lambda_{s,1}}(\boldsymbol{t}_1 - \beta_1\boldsymbol{d}_1)$) is known since β_1 and $\boldsymbol{d}_1$ are known, and $\boldsymbol{w}_1$ is just recovered. Thus, $\boldsymbol{\theta}_{1,k}$ and $\boldsymbol{w}_{1,k}$ can be pre-cancelled from $\boldsymbol{\delta}_{m,k}$ as follows. Let $\boldsymbol{t}_l = (\bar{\varphi}(\boldsymbol{w}_1)) \bmod \Lambda_{s,1}$. Then, $\boldsymbol{\theta}_{1,k}$ can be obtained from $\varphi(\boldsymbol{t}_1 - \beta_1\boldsymbol{d}_1))$ and $\boldsymbol{w}_{1,k}$ can be obtained from $\varphi(\boldsymbol{t}_1)$. Then, for $m \in \mathcal{M}_k$,

$$\begin{aligned}
&\big(\boldsymbol{\delta}_{m,k} + a_{m1}(\boldsymbol{\theta}_{1,k} - \boldsymbol{w}_{1,k})\big) \bmod q & (128a)\\
&= \big(\boldsymbol{u}_{m,k} + a_{m1}(\boldsymbol{\theta}_{1,k} - \boldsymbol{w}_{1,k})\big) \bmod q & (128b)\\
&= \left(\sum_{l\in\mathcal{L}_k} a_{ml}\boldsymbol{w}_{l,k} - a_{m1}(\boldsymbol{\theta}_{1,k} - \boldsymbol{w}_{1,k}) + a_{m1}(\boldsymbol{\theta}_{1,k} - \boldsymbol{w}_{1,k})\right) \bmod q & (128c)\\
&= \left(\sum_{l\in\mathcal{L}_k} a_{ml}\boldsymbol{w}_{l,k}\right) \bmod \Lambda_k & (128d)
\end{aligned}$$

where (128b) is from (122), (128c) is from (127). Then, following the approach in (124) and (125), we can recover $\{\boldsymbol{w}_{l,k}|l \in \mathcal{L}_k\}$ for $k = \pi(1)-1$.

Note that $\Lambda_{s,2} = \Lambda_{\pi(3)}$. Then, (126) still holds for $\pi(3) \leq k \leq \pi(1)-2$. Thus, following the approach in (127)-(128), we can recover $\{\boldsymbol{w}_{l,k}|l \in \mathcal{L}_k\}$ for $\pi(3) \leq k \leq \pi(1)-2$ in the same way. Recall from (44) that $\mathcal{K}_2 = \{k|\pi(3) \leq k \leq \pi(5)\} \subseteq \{k|\pi(3) \leq k \leq 2L-1\}$. Therefore, we can also recover $\boldsymbol{w}_2$ by (45).

By induction, we can recover $\{\boldsymbol{w}_l\}_1^L$ recursively. This completes the proof.

APPENDIX D
PROOF OF THEOREM 2

We first show (68). The compression function in (58) gives a bijection between $\boldsymbol{\delta}_m$ and $\{\boldsymbol{u}_{m,k}|k \in \mathcal{J}_{\pi_\alpha^{-1}(m)}\}$. Thus,

$$H(\boldsymbol{\delta}_m) = H(\boldsymbol{u}_{m,k}|k \in \mathcal{J}_{\pi_\alpha^{-1}(m)}). \tag{129}$$

To prove (68), it suffices to show that

$$\frac{1}{n}H(\boldsymbol{u}_{m,k}) = r_{v,k} \tag{130}$$

[4]For the example in Fig. 7, $\pi(1)-1 = 2$.

and $\boldsymbol{u}_{m,k}$ is independent of $\boldsymbol{u}_{m,k'}$ for any $k \neq k'$ and $k,k' \in \mathcal{J}_{\pi_\alpha^{-1}(m)}$, i.e.,

$$H(\boldsymbol{u}_{m,k}|k \in \mathcal{J}_{\pi_\alpha^{-1}(m)}) = \sum_{k\in\mathcal{J}_{\pi_\alpha^{-1}(m)}} H(\boldsymbol{u}_{m,k}). \tag{131}$$

Recall that $\boldsymbol{u}_{m,k}$ is given by (54). Note that $\{a_{m,l}|l \in \mathcal{L}_k\}$ defines $\boldsymbol{A}(m,\mathcal{L}_k)$. Also note that the submatrix $\boldsymbol{A}(\overline{\mathcal{I}_{m-1}},\mathcal{L}_k)$ has one more row (i.e. $\boldsymbol{A}(m,\mathcal{L}_k)$) than the submatrix $\boldsymbol{A}(\overline{\mathcal{I}_m},\mathcal{L}_k)$. Then, from the definition in (57), for $k \in \mathcal{J}_{\pi_\alpha^{-1}(m)}$, $\boldsymbol{A}(m,\mathcal{L}_k)$ can not be a zero vector, and so $\{a_{m,l}|l \in \mathcal{L}_k\}$ are not all zeros. From Lemma 4, $\boldsymbol{u}_{m,k}$ is uniformly distributed over $\mathbb{Z}_q^{i_{k+1}-i_k}$ and is also independent of $\boldsymbol{u}_{m,k'}$ for $k \neq k'$ and $k,k' \in \mathcal{J}_{\pi_\alpha^{-1}(m)}$. Therefore, we have

$$\frac{1}{n}H(\boldsymbol{u}_{m,k}) = r_{v,k}, \tag{132}$$

and

$$\begin{aligned}
\frac{1}{n}H(\boldsymbol{\delta}_m) &= \frac{1}{n}H(\boldsymbol{u}_{m,k}|k \in \mathcal{J}_{\pi_\alpha^{-1}(m)}) & (133a)\\
&= \frac{1}{n}\sum_{k\in\mathcal{J}_{\pi_\alpha^{-1}(m)}} H(\boldsymbol{u}_{m,k}) & (133b)\\
&= \sum_{k\in\mathcal{J}_{\pi_\alpha^{-1}(m)}} r_{v,k}. & (133c)
\end{aligned}$$

We then show (69). The left hand side (LHS) of (69) can be represented as

$$\begin{aligned}
\frac{1}{n}\sum_{m=1}^{L} H(\boldsymbol{\delta}_m) &= \frac{1}{n}\sum_{m=1}^{L}\sum_{k\in\mathcal{J}_{\pi_\alpha^{-1}(m)}} H(\boldsymbol{\delta}_{m,k}) & (134a)\\
&= \frac{1}{n}\sum_{k=1}^{2L-1}\sum_{m\in\mathcal{M}_k} H(\boldsymbol{\delta}_{m,k}) & (134b)\\
&= \sum_{k=1}^{2L-1} |\mathcal{M}_k| r_{v,k} & (134c)\\
&= \sum_{k=1}^{2L-1} |\mathcal{L}_k| r_{v,k} & (134d)
\end{aligned}$$

where (134a) is from (133b) together with $\boldsymbol{\delta}_{\pi_\alpha(m),k} = \boldsymbol{u}_{\pi_\alpha(m),k}$ for $k \in \mathcal{J}_{\pi_\alpha(m)}$ and $\boldsymbol{\delta}_{\pi_\alpha(m),k} = \boldsymbol{0}$ for $k \notin \mathcal{J}_{\pi_\alpha(m)}$, (134b) is from the definition of $\mathcal{M}_k$ in (121). The RHS of (69) can be represented as

$$\begin{aligned}
\sum_{l=1}^{L} r_l &= \frac{1}{n}H(\{\boldsymbol{w}_l|l \in \mathcal{I}_L\}) & (135a)\\
&= \frac{1}{n}H(\{\boldsymbol{w}_{l,k}|l \in \mathcal{I}_L, k \in \mathcal{K}_l\}) & (135b)\\
&= \frac{1}{n}H(\{\boldsymbol{w}_{l,k}|l \in \mathcal{L}_k, k \in \mathcal{I}_{2L-1}\}) & (135c)\\
&= \sum_{k=1}^{2L-1} |\mathcal{L}_k| r_{v,k}. & (135d)
\end{aligned}$$

By combining (134) and (135), we obtain (69).

APPENDIX E
PROOF OF THEOREM 5

To prove Theorem 5, we need to show that (79) holds for $L = 2$. The RHS of (79) can be represented as

$$H\left(\{\boldsymbol{v}_m|m\in\mathcal{S}\}|\{\boldsymbol{v}_m|m\in\overline{\mathcal{S}}\}\right)=H\left(\boldsymbol{v}_m|m\in\mathcal{I}_L\right)-H\left(\boldsymbol{v}_m|m\in\overline{\mathcal{S}}\right). \tag{136}$$

Thus, we need to show that

$$\frac{1}{n}H\left(\{\boldsymbol{v}_m|m\in\mathcal{S}\}\right)=\sum_{k=1}^{2L-1}rank(\boldsymbol{A}(\mathcal{S},\mathcal{L}_k))r_{\mathrm{v},k},\quad \text{for } \mathcal{S}\in\mathcal{I}_2. \tag{137}$$

From the fact $\boldsymbol{v}_m\in\Lambda_{2L}\cap\mathcal{V}_1$ and Lemma 2, $H\left(\{\boldsymbol{v}_m|m\in\mathcal{S}\}\right)=H\left(\{\boldsymbol{u}_m|m\in\mathcal{S}\}\right)$. Thus, to show (137), it suffices to show

$$\frac{1}{n}H\left(\{\boldsymbol{u}_m|m\in\mathcal{S}\}\right)=\sum_{k=1}^{2L-1}rank(\boldsymbol{A}(\mathcal{S},\mathcal{L}_k))r_{\mathrm{v},k},\quad \text{for } \mathcal{S}\in\mathcal{I}_2. \tag{138}$$

The non-empty subsets of $\mathcal{I}_2$ are given by $\{1\},\{2\},\mathcal{I}_2$. For $\mathcal{S}=\mathcal{I}_2$, we have

$$\frac{1}{n}H\left(\{\boldsymbol{u}_m|m\in\mathcal{S}\}\right)=\frac{1}{n}H(\boldsymbol{t}_1,\boldsymbol{t}_2) \tag{139a}$$
$$=\sum_{k=1}^{2L-1}|\mathcal{L}_k|r_{\mathrm{v},k} \tag{139b}$$

where (139a) follows from the fact that $\{\boldsymbol{t}_1,\boldsymbol{t}_2\}$ can be recovered from $\{\boldsymbol{u}_1,\boldsymbol{u}_2\}$, and (139b) from (135). Note that for $\mathcal{S}=\mathcal{I}_2$, $rank(\boldsymbol{A}(\mathcal{S},\mathcal{L}_k))=|\mathcal{L}_k|$. Thus, (137) holds for $\mathcal{S}=\mathcal{I}_2$.

We now prove (137) for $\mathcal{S}=\{1\}$. The proof for $\mathcal{S}=\{2\}$ is similar and thus omitted. By the chain rule of the entropy,

$$\begin{aligned}H(\boldsymbol{u}_1)&=H(\boldsymbol{u}_{1,1},\boldsymbol{u}_{1,2},\boldsymbol{u}_{1,3})\\&=H(\boldsymbol{u}_{1,3})+H(\boldsymbol{u}_{1,2}|\boldsymbol{u}_{1,3})+H(\boldsymbol{u}_{1,1}|\boldsymbol{u}_{1,2},\boldsymbol{u}_{1,3}).\end{aligned} \tag{140}$$

With (140), to prove (138), it suffices to show

$$\frac{1}{n}H(\boldsymbol{u}_{1,k}|\{\boldsymbol{u}_{1,k'}\}_{k'=k+1}^{3})=rank(\boldsymbol{A}(1,\mathcal{L}_k))r_{\mathrm{v},k},\quad \text{for } k\in\mathcal{I}_3. \tag{141}$$

where $\{\boldsymbol{u}_{1,k'}\}_{k'=k+1}^{3}=\emptyset$ if $k+1>3$. If $\boldsymbol{A}(1,\mathcal{L}_k)\neq\boldsymbol{0}$, from Lemma 4, we have $\boldsymbol{u}_{1,k}$ is independent of $\{\boldsymbol{u}_{1,k'}$ for $k'>k$, and thus

$$\frac{1}{n}H(\boldsymbol{u}_{1,k}|\{\boldsymbol{u}_{1,k'}\}_{k'=k+1}^{3})=\frac{1}{n}H(\boldsymbol{u}_{1,k}) \tag{142a}$$
$$=r_{\mathrm{v},k} \tag{142b}$$
$$=rank(\boldsymbol{A}(1,\mathcal{L}_k))r_{\mathrm{v},k}. \tag{142c}$$

If $\boldsymbol{A}(1,\mathcal{L}_k)=\boldsymbol{0}$, we have $[a_{1l}]\triangleq\boldsymbol{A}(1,\mathcal{I}_2/\mathcal{L}_k)\neq\boldsymbol{0}$ since $\boldsymbol{A}$ is invertible, where $\{l\}=\mathcal{I}_2/\mathcal{L}_k$. From (55) and (44), since $l\notin\mathcal{L}_k$, we have $k\notin\mathcal{K}_l$. In the following, we show (141) for $k=3,2,1$ with $\boldsymbol{A}(1,\mathcal{L}_k)=\boldsymbol{0}$ holding.

For $k=3$, then $k>\max\{\mathcal{K}_l\}$. From (56), we have $\boldsymbol{u}_{1,3}=a_{1l}\boldsymbol{w}_{l,3}$. From (42), we have $\boldsymbol{w}_{l,3}=\boldsymbol{0}$. Thus,

$$\frac{1}{n}H(\boldsymbol{u}_{1,3})=\frac{1}{n}H(\boldsymbol{0})=0=rank(\boldsymbol{A}(1,\mathcal{L}_k))r_{\mathrm{v},k}. \tag{143}$$

For $k=2$, then $k>\max\{\mathcal{K}_l\}$ or $k<\min\{\mathcal{K}_l\}$. If $k>\max\{\mathcal{K}_l\}$, following the derivation in the case of $k=3$, we obtain

$$\frac{1}{n}H(\boldsymbol{u}_{1,2}|\boldsymbol{u}_{1,3})=rank(\boldsymbol{A}(1,\mathcal{L}_k))r_{\mathrm{v},k}. \tag{144}$$

If $k<\min\{\mathcal{K}_l\}$, then $\mathcal{K}_l=\{3\}$. From Lemma 3, $\tilde{\boldsymbol{w}}_l=\tilde{\boldsymbol{w}}_{l,3}$. Thus,

$$\frac{1}{n}H(\boldsymbol{u}_{1,2}|\boldsymbol{u}_{1,3})=\frac{1}{n}H(a_{1l}(\boldsymbol{w}_{l,2}-\boldsymbol{\theta}_{l,2})|a_{1l}\boldsymbol{w}_{l,3}) \tag{145a}$$
$$=\frac{1}{n}H(\boldsymbol{w}_{l,2}-\boldsymbol{\theta}_{l,2}|\boldsymbol{w}_l) \tag{145b}$$
$$=0 \tag{145c}$$
$$=rank(\boldsymbol{A}(1,\mathcal{L}_k))r_{\mathrm{v},k}, \tag{145d}$$

where (145c) follows from the fact that $\boldsymbol{t}_l$ is determined by $\tilde{\boldsymbol{w}}_l$ and thus $\boldsymbol{w}_{l,2}$ and $\boldsymbol{\theta}_{l,2}$ are determined by $\boldsymbol{t}_l$.

For $k=1$, then $k<\min\{\mathcal{K}_l\}$. Following the derivation in the case of $k=2$, we have

$$\frac{1}{n}H(\boldsymbol{u}_{1,1}|\boldsymbol{u}_{1,2},\boldsymbol{u}_{1,3})=rank(\boldsymbol{A}(1,\mathcal{L}_k))r_{\mathrm{v},k}. \tag{146}$$

This concludes the proof.

APPENDIX F
PROOF OF THEOREM 6

We prove Theorem 6 by showing that if all the transmitters share a common shaping lattice, i.e. $\Lambda_{\mathrm{s},1}=\cdots=\Lambda_{\mathrm{s},L}$, GCCF achieves the vertices of $\mathcal{R}_{SW}$. The following lemma gives the vertices of $\mathcal{R}_{\mathrm{SW}}$.

Lemma 6: The vertex of $\mathcal{R}_{SW}$ specified by $\pi_\alpha(\cdot)$ is given by $(R_1,R_2,\cdots,R_L)$ with

$$R_{\pi_\alpha(m)}=\frac{1}{n}H\left(\boldsymbol{v}_{\pi_\alpha(m)}|\{\boldsymbol{v}_i,i\in\Pi_\alpha(\overline{\mathcal{I}_m})\}\right),\quad \text{for } m\in\mathcal{I}_L. \tag{147}$$

Proof: We follow the proof of Theorem 3. Note that the vertices of $\mathcal{R}_{SW}$ is also given by the weighted sum-rate minimization problem given in (75) with $f(\mathcal{S})$ replaced by

$$h(\mathcal{S})\triangleq\frac{1}{n}H\left(\{\boldsymbol{v}_m|m\in\mathcal{S}\}|\{\boldsymbol{v}_m|m\in\overline{\mathcal{S}}\}\right),\quad \text{for } \mathcal{S}\subseteq\mathcal{I}_L. \tag{148}$$

Also note that $-h(\mathcal{S})$ is a submodular function since the entropy function is submodular [33, pp. 31]. Thus, similar to (76), we have

$$R_{\pi_\alpha(m)}=h(\Pi_\alpha(\mathcal{I}_m))-h(\Pi_\alpha(\mathcal{I}_{m-1})) \tag{149a}$$
$$=\frac{1}{n}H\left(\{\boldsymbol{v}_m|m\in\Pi_\alpha(\overline{\mathcal{I}_{m-1}})\}\right)-\frac{1}{n}H\left(\{\boldsymbol{v}_m|m\in\Pi_\alpha(\overline{\mathcal{I}_m})\}\right) \tag{149b}$$
$$=\frac{1}{n}H\left(\boldsymbol{v}_{\pi_\alpha(m)}|\{\boldsymbol{v}_i,i\in\Pi_\alpha(\overline{\mathcal{I}_m})\}\right) \tag{149c}$$

where (149b) follows from (148) and the chain rule of the entropy. ■

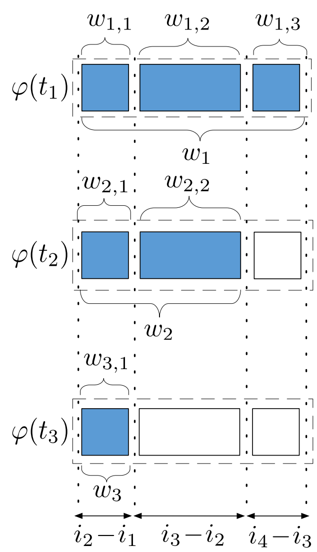

Fig. 12. The label splitting for $\{\varphi(\boldsymbol{t}_l)\}_{l=1}^{3}$ under the assumption of $\Lambda_{s,1} = \cdots = \Lambda_{s,L}$.

By assumption, $\boldsymbol{v}_m$ in (23) reduces to

$$\boldsymbol{v}_m = \left(\sum_{l=1}^{L} a_{ml}(\boldsymbol{t}_l - Q_{\Lambda_{s,l}}(\boldsymbol{t}_l - \beta_l \boldsymbol{d}_l))\right) \bmod \Lambda_1 \tag{150}$$

$$= \left(\sum_{l=1}^{L} a_{ml}(\boldsymbol{t}_l - Q_{\Lambda_{s,l}}(\boldsymbol{t}_l - \beta_l \boldsymbol{d}_l) \bmod \Lambda_1)\right) \bmod \Lambda_1 \tag{151}$$

$$= \left(\sum_{l=1}^{L} a_{ml}\boldsymbol{t}_l\right) \bmod \Lambda_1. \tag{152}$$

Then, $\boldsymbol{u}_m$ and the k-th message segment of $\boldsymbol{u}_m$ reduces to

$$\boldsymbol{u}_m = \left(\sum_{l=1}^{L} a_{ml}\varphi(\boldsymbol{t}_l)\right) \bmod q. \tag{153}$$

Following (56), the k-th message segment of $\boldsymbol{u}_m$ is given by

$$\boldsymbol{u}_{m,k} = \left(\sum_{l\in\mathcal{L}_k} a_{ml}\boldsymbol{w}_{l,k}\right) \bmod q. \tag{154}$$

Note that under the assumption, the nested lattice chain is given by

$$\Lambda_1 \subseteq \Lambda_2 \subseteq \cdots \subseteq \Lambda_{L+1} \tag{155}$$

where Λ_1 serves as the common shaping lattice and $\{\Lambda_k\}_{k=2}^{L+1}$ serve as the L coding lattices. Then, there are L message segments in $\varphi(\boldsymbol{t}_l)$ and $\boldsymbol{u}_m$ (not $2L-1$ anymore). A illustration of label splitting for $\{\varphi(\boldsymbol{t}_l)\}$ is given by Fig. 12.

From Theorem 2, the achievable rate tuples of GCCF are given by (68). Thus, together with Lemma 6, to prove Theorem 6, it suffices to show that

$$H(\boldsymbol{\delta}_{\pi_\alpha(m)}) = H\left(\boldsymbol{v}_{\pi_\alpha(m)}|\{\boldsymbol{v}_i, i\in\Pi_\alpha(\overline{\mathcal{I}_m})\}\right), \quad \text{for } m\in\mathcal{I}_L. \tag{156}$$

From the fact $\boldsymbol{v}_m \in \Lambda_{2L}\cap\mathcal{V}_1$ and Lemma 2, $H(\{\boldsymbol{v}_m|m\in\mathcal{S}\}) = H(\{\boldsymbol{u}_m|m\in\mathcal{S}\})$, to show (156), it suffices to show

$$H(\boldsymbol{\delta}_{\pi_\alpha(m)}) = H\left(\boldsymbol{u}_{\pi_\alpha(m)}|\{\boldsymbol{u}_i, i\in\Pi_\alpha(\overline{\mathcal{I}_m})\}\right), \quad \text{for } m\in\mathcal{I}_L. \tag{157}$$

From (133b), the LHS of (157) can be represented as

$$H(\boldsymbol{\delta}_{\pi_\alpha(m)}) = \sum_{k\in\mathcal{J}_m} H(\boldsymbol{u}_{\pi_\alpha(m),k}). \tag{158}$$

The RHS of (157) can be written as

$$\begin{aligned} & H\left(\boldsymbol{u}_{\pi_\alpha(m)}|\{\boldsymbol{u}_i, i\in\Pi_\alpha(\overline{\mathcal{I}_m})\}\right) && (159a)\\ &= H\left(\{\boldsymbol{u}_{\pi_\alpha(m),k}\}_{k=1}^{2L-1}|\{\boldsymbol{u}_i, i\in\Pi_\alpha(\overline{\mathcal{I}_m})\}\right) && (159b)\\ &= H\left(\boldsymbol{u}_{\pi_\alpha(m),1}|\{\boldsymbol{u}_i, i\in\Pi_\alpha(\overline{\mathcal{I}_m})\}, \{\boldsymbol{u}_{\pi_\alpha(m),k}\}_{k=2}^{L}\right)\\ &\quad + H\left(\boldsymbol{u}_{\pi_\alpha(m),2}|\{\boldsymbol{u}_i, i\in\Pi_\alpha(\overline{\mathcal{I}_m})\}, \{\boldsymbol{u}_{\pi_\alpha(m),k}\}_{k=3}^{L}\right)\\ &\quad + \cdots + H\left(\boldsymbol{u}_{\pi_\alpha(m),L}|\{\boldsymbol{u}_i, i\in\Pi_\alpha(\overline{\mathcal{I}_m})\}\right) && (159c)\end{aligned}$$

where (159b) is from the bijection between $\boldsymbol{u}_m$ and $\{\boldsymbol{u}_{m,k}\}_{k=1}^{L}$, and (159c) is from the chain rule of the entropy. To ensure (157), it suffices to show

$$\begin{aligned} & H\left(\boldsymbol{u}_{\pi_\alpha(m),k}|\{\boldsymbol{u}_i, i\in\Pi_\alpha(\overline{\mathcal{I}_m})\}, \{\boldsymbol{u}_{\pi_\alpha(m),k'}\}_{k'=k+1}^{L}\right)\\ &\quad = 0, \quad \text{for } k\notin\mathcal{J}_m && (160a)\\ & H\left(\boldsymbol{u}_{\pi_\alpha(m),k}|\{\boldsymbol{u}_i, i\in\Pi_\alpha(\overline{\mathcal{I}_m})\}, \{\boldsymbol{u}_{\pi_\alpha(m),k'}\}_{k'=k+1}^{L}\right)\\ &\quad = H(\boldsymbol{u}_{\pi_\alpha(m),k}), \quad \text{for } k\in\mathcal{J}_m && (160b)\end{aligned}$$

where $\{\boldsymbol{v}_{\pi_\alpha(m),k'}\}_{k'=k+1}^{L} = \emptyset$ for $k+1 > L$. In the following, we show (160) according to the case $A(\pi_\alpha(m),\mathcal{L}_k) = \boldsymbol{0}$ and the case $A(\pi_\alpha(m),\mathcal{L}_k) \neq \boldsymbol{0}$.

If $A(\pi_\alpha(m),\mathcal{L}_k) = \boldsymbol{0}$, from (154), we have $\boldsymbol{u}_{\pi_\alpha(m),k} = \boldsymbol{0}$. Then, (160a) and (160b) hold.

If $A(\pi_\alpha(m),\mathcal{L}_k) \neq \boldsymbol{0}$, $\boldsymbol{u}_{m,k}$ is independent of $\{\boldsymbol{u}_{m',k'}|m'\in\mathcal{I}_L, k'\in\mathcal{I}_L\backslash\{k\}\}$ (since $\boldsymbol{u}_{m,k}$ is a linear combination of $\{\boldsymbol{w}_{l,k}\}$ and $\boldsymbol{w}_{l,k}$ is independent of $\boldsymbol{w}_{l,k'}$ for $k\neq k'$). Then, the LHS of (160a) can be represented as

$$\begin{aligned} & H\left(\boldsymbol{u}_{\pi_\alpha(m),k}|\{\boldsymbol{u}_i, i\in\Pi_\alpha(\overline{\mathcal{I}_m})\}, \{\boldsymbol{u}_{\pi_\alpha(m),k'}\}_{k'=k+1}^{L}\right)\\ &= H\left(\boldsymbol{u}_{\pi_\alpha(m),k}|\{\{\boldsymbol{u}_{i,k'}, i\in\Pi_\alpha(\overline{\mathcal{I}_m})\}\}_{k'=1}^{2L-1}, \{\boldsymbol{u}_{\pi_\alpha(m),k'}\}_{k'=k+1}^{L}\right)\\ &= H\left(\boldsymbol{u}_{\pi_\alpha(m),k}|\{\boldsymbol{u}_{i,k}, i\in\Pi_\alpha(\overline{\mathcal{I}_m})\}\right).\end{aligned}$$

Thus, (160) reduces to

$$H\left(\boldsymbol{u}_{\pi_\alpha(m),k}|\{\boldsymbol{u}_{i,k}, i\in\Pi_\alpha(\overline{\mathcal{I}_m})\}\right) = 0, \quad \text{for } k\notin\mathcal{J}_m, \tag{161a}$$

$$H\left(\boldsymbol{u}_{\pi_\alpha(m),k}|\{\boldsymbol{u}_{i,k}, i\in\Pi_\alpha(\overline{\mathcal{I}_m})\}\right) = H(\boldsymbol{u}_{\pi_\alpha(m),k}), \quad \text{for } k\in\mathcal{J}_m. \tag{161b}$$

To show (161), it suffices to show that $\boldsymbol{v}_{\pi_\alpha(m),k}$ is deterministic given $\{\boldsymbol{v}_{i,k}, i\in\Pi_\alpha(\overline{\mathcal{I}_m})\}$ for $k\notin\mathcal{J}_m$ and $\boldsymbol{v}_{\pi_\alpha(m),k}$ is independent of $\{\boldsymbol{v}_{i,k}, i\in\Pi_\alpha(\overline{\mathcal{I}_m})\}$ for $k\in\mathcal{J}_m$.

Note that $k\notin\mathcal{J}_m$ can be interpreted as : $\boldsymbol{A}(\pi_\alpha(m),\mathcal{L}_k)$ is linear dependent of the rows of $\boldsymbol{A}(\pi_\alpha(\overline{\mathcal{I}_m}),\mathcal{L}_k)$ and $k\in\mathcal{J}_m$ can be interpreted as : $\boldsymbol{A}(\pi_\alpha(m),\mathcal{L}_k)$ is linear independent of the rows of $\boldsymbol{A}(\pi_\alpha(\overline{\mathcal{I}_m}),\mathcal{L}_k)$. Therefore, the proof of Theorem 6 concludes by the following Lemma.

Lemma 7: For the message segment $\boldsymbol{v}_{m,k}$ in (154), $\boldsymbol{u}_{m,k}$ is deterministic given $\{\boldsymbol{u}_{m',k}|m'\in\mathcal{S}\}$ if $\boldsymbol{A}(m,\mathcal{L}_k)$ is linearly dependent of the row vectors of $\boldsymbol{A}(\mathcal{S},\mathcal{L}_k)$; otherwise, $\boldsymbol{v}_{m,k}$ is independent of $\{\boldsymbol{u}_{m',k}|m' \in \mathcal{S}\}$ if $\boldsymbol{A}(m,\mathcal{L}_k)$ is linearly independent of the row vectors of $\boldsymbol{A}(\mathcal{S},\mathcal{L}_k)$.

Proof: Following the approach in Appendix C, we take transpose on the both sides of (154) and then stacking the result row by row for $m' \in \Pi_\alpha(\overline{\mathcal{I}_{m-1}})$, we obtain

$$\begin{bmatrix} \boldsymbol{u}^{\mathrm{T}}_{\pi_\alpha(m),k} \\ \boldsymbol{u}^{\mathrm{T}}_{\pi_\alpha(m+1),k} \\ \vdots \\ \boldsymbol{u}^{\mathrm{T}}_{\pi_\alpha(L),k} \end{bmatrix} = \begin{bmatrix} \boldsymbol{A}(\pi_\alpha(m),\mathcal{L}_k) \\ \boldsymbol{A}(\Pi_\alpha(\overline{\mathcal{I}_m}),\mathcal{L}_k) \end{bmatrix} \begin{bmatrix} \boldsymbol{w}^{\mathrm{T}}_{l_1,k} \\ \boldsymbol{w}^{\mathrm{T}}_{l_2,k} \\ \vdots \\ \boldsymbol{w}^{\mathrm{T}}_{l_{|\mathcal{L}_k|},k}. \end{bmatrix} \quad (162)$$

where $\bar{\boldsymbol{v}}_{\pi_\alpha(m'),k} \triangleq (\phi^{-1}_{\mathrm{v},k}(\boldsymbol{v}_{m',k}))$.

We first consider the case that $\boldsymbol{A}(\pi_\alpha(m),\mathcal{L}_k)$ is linearly dependent of $\boldsymbol{A}(\Pi_\alpha(\overline{\mathcal{I}_m}),\mathcal{L}_k)$. Then, $\boldsymbol{A}(\pi_\alpha(m),\mathcal{L}_k)$ can be represented by a linear combination of $\boldsymbol{A}(\pi_\alpha(\overline{\mathcal{I}_m}),\mathcal{L}_k)$. Thus, $\boldsymbol{u}_{\pi_\alpha(m),k}$ can also be represented by a linear combination of $\{\boldsymbol{u}_{i,k}, i \in \pi_\alpha(\overline{\mathcal{I}_m})\}$. Therefore, $\bar{\boldsymbol{v}}_{\pi_\alpha(m),k}$ is deterministic for given $\{\bar{\boldsymbol{v}}_{i,k}, i \in \pi_\alpha(\overline{\mathcal{I}_m})\}$ and so $\boldsymbol{v}_{\pi_\alpha(m),k}$ is deterministic for given $\{\boldsymbol{v}_{i,k}, i \in \pi_\alpha(\overline{\mathcal{I}_m})\}$.

We next consider the case that $\boldsymbol{A}(\pi_\alpha(m),\mathcal{L}_k)$ is linearly independent of $\boldsymbol{A}(\Pi_\alpha(\overline{\mathcal{I}_m}),\mathcal{L}_k)$. By reducing $\boldsymbol{A}(\Pi_\alpha(\overline{\mathcal{I}_m}),\mathcal{L}_k)$ into row reducing echelon form, we obtain

$$\begin{bmatrix} \boldsymbol{u}'^{\mathrm{T}}_{\pi_\alpha(m+1),k} \\ \boldsymbol{u}'^{\mathrm{T}}_{\pi_\alpha(m+2),k} \\ \vdots \\ \boldsymbol{u}'^{\mathrm{T}}_{\pi_\alpha(L),k} \end{bmatrix} = \begin{bmatrix} \boldsymbol{I}_\lambda & \boldsymbol{F} \\ \boldsymbol{0} & \boldsymbol{0} \end{bmatrix} \begin{bmatrix} \boldsymbol{w}^{\mathrm{T}}_{l_1,k} \\ \boldsymbol{w}^{\mathrm{T}}_{l_2,k} \\ \vdots \\ \boldsymbol{w}^{\mathrm{T}}_{l_{|\mathcal{L}_k|},k} \end{bmatrix}. \quad (163)$$

where λ is the rank of $\boldsymbol{A}(\Pi_\alpha(\overline{\mathcal{I}_m}),\mathcal{L}_k)$, $\boldsymbol{F}$ is the free matrix, and $\boldsymbol{u}'^{\mathrm{T}}_{\pi_\alpha(m'),k}$ are obtained from $\boldsymbol{u}^{\mathrm{T}}_{\pi_\alpha(m'),k}$ by the row operations that transforms $\boldsymbol{A}(\Pi_\alpha(\overline{\mathcal{I}_m}),\mathcal{L}_k)$ into $[\boldsymbol{I}_\lambda,\boldsymbol{F};\boldsymbol{0},\boldsymbol{0}]$. Note that the linear transform from $\{\bar{\boldsymbol{v}}^{\mathrm{T}}_{\pi_\alpha(m'),k}\}$ to $\{\bar{\boldsymbol{v}}'^{\mathrm{T}}_{\pi_\alpha(m'),k}\}$ is invertible. From (163), we have

$$\begin{bmatrix} \boldsymbol{w}^{\mathrm{T}}_{l_1,k} \\ \boldsymbol{w}^{\mathrm{T}}_{l_2,k} \\ \vdots \\ \boldsymbol{w}^{\mathrm{T}}_{l_\lambda,k}. \end{bmatrix} = \begin{bmatrix} \boldsymbol{u}'^{\mathrm{T}}_{\pi_\alpha(m+1),k} \\ \boldsymbol{u}'^{\mathrm{T}}_{\pi_\alpha(m+2),k} \\ \vdots \\ \boldsymbol{u}'^{\mathrm{T}}_{\pi_\alpha(m+\lambda),k} \end{bmatrix} - \boldsymbol{F} \begin{bmatrix} \boldsymbol{w}^{\mathrm{T}}_{l_{\lambda+1},k} \\ \boldsymbol{w}^{\mathrm{T}}_{l_2,k} \\ \vdots \\ \boldsymbol{w}^{\mathrm{T}}_{l_{|\mathcal{L}_k|},k} \end{bmatrix}. \quad (164)$$

Thus, we can represent $\boldsymbol{u}_{\pi_\alpha(m),k}$ as a linear combination of $\{\boldsymbol{u}_{\pi_\alpha(m'),k}, m' \in \Pi_\alpha(\overline{\mathcal{I}_m})\}$ and $\{\boldsymbol{w}_{l_i,k}, l_i \in \{l_{\lambda+1},\cdots,l_{|\mathcal{L}_k|}\}\}$.

From the assumption that $\boldsymbol{A}(\pi_\alpha(m),\mathcal{L}_k)$ is linearly independent of the rows of $\boldsymbol{A}(\Pi_\alpha(\overline{\mathcal{I}_m}),\mathcal{L}_k)$, the coefficients of $\{\boldsymbol{w}_{l_i,k}, l_i \in \{l_{\lambda+1},\cdots,l_{|\mathcal{L}_k|}\}\}$ are not all-zero; otherwise, $\boldsymbol{u}_{\pi_\alpha(m),k}$ is a linear combination of $\{\boldsymbol{u}'_{\pi_\alpha(m'),k}, m' \in \Pi_\alpha(\overline{\mathcal{I}_m})\}$, which contradicts to the assumption. By following the proof in Lemma 4, it can be shown that $\boldsymbol{u}_{\pi_\alpha(m),k}$ is independent of $\{\boldsymbol{u}_{i,k}, i \in \Pi_\alpha(\overline{\mathcal{I}_m})\}$, which concludes the proof of Lemma 7. ■

References

[1] B. Nazer and M. Gastpar, "Compute-and-forward: Harnessing interference through structured codes," *IEEE Trans. Inf. Theory*, vol. 57, no. 10, pp. 6463–6486, Oct. 2011.

[2] U. Erez and R. Zamir, "Achieving 1/2 log (1+SNR) on the AWGN channel with lattice encoding and decoding," *IEEE Trans. Inf. Theory*, vol. 50, no. 10, pp. 2293–2314, Oct. 2004.

[3] V. Ntranos, V. R. Cadambe, B. Nazer, and G. Caire, "Asymmetric compute-and-forward," in *Proc. 51st Annu. Allerton Conf. Commun., Control, Comput. (Allerton)*, Monticello, IL, USA, Oct. 2013, pp. 1174–1181.

[4] J. Zhu and M. Gastpar, "Lattice codes for many-to-one interference channels with and without cognitive messages," *IEEE Trans. Inf. Theory*, vol. 61, no. 3, pp. 1309–1324, Mar. 2015.

[5] B. Nazer, V. R. Cadambe, V. Ntranos, and G. Caire, "Expanding the compute-and-forward framework: Unequal powers, signal levels, and multiple linear combinations," *IEEE Trans. Inf. Theory*, vol. 62, no. 9, pp. 4879–4909, Sep. 2016.

[6] B. Nazer, "Successive compute-and-forward," in *Proc. 22nd Int. Zürich Seminar Commun. (IZS)*, Zürich, Switzerland, Mar. 2012, pp. 103–106.

[7] O. Ordentlich, U. Erez, and B. Nazer, "Successive integer-forcing and its sum-rate optimality," in *Proc. 51st Annu. Allerton Conf. Commun., Control, Comput.*, Allerton, IL, USA, 2013, pp. 282–292.

[8] U. Niesen and P. Whiting, "The degrees of freedom of compute-and-forward," *IEEE Trans. Inf. Theory*, vol. 58, no. 8, pp. 5214–5232, Aug. 2012.

[9] Y. Tan and X. Yuan, "Compute-compress-and-forward: Exploiting asymmetry of wireless relay networks," *IEEE Trans. Signal Process.*, vol. 64, no. 2, pp. 511–524, Jan. 2016.

[10] Y. Tan, X. Yuan, S. C. Liew, and A. Kavcic, "Asymmetric compute-and-forward: Going beyond one hop," in *Proc. 52nd Annu. Allerton Conf. Commun., Control, Comput.*, Allerton, IL, USA, Sep./Oct. 2014, pp. 667–674.

[11] J. Zhan, B. Nazer, U. Erez, and M. Gastpar, "Integer-forcing linear receivers," *IEEE Trans. Inf. Theory*, vol. 60, no. 12, pp. 7661–7685, Dec. 2014.

[12] T. Yang, X. Yuan, and Q. T. Sun, "A signal-space aligned network coding approach to distributed MIMO," *IEEE Trans. Signal Process.*, vol. 65, no. 1, pp. 27–40, Jan. 2017.

[13] W. Nam, S.-Y. Chung, and Y. H. Lee, "Capacity of the Gaussian two-way relay channel to within 1/2 bit," *IEEE Trans. Inf. Theory*, vol. 56, no. 11, pp. 5488–5494, Nov. 2010.

[14] W. Nam, S.-Y. Chung, and Y. H. Lee, "Nested lattice codes for Gaussian relay networks with interference," *IEEE Trans. Inf. Theory*, vol. 57, no. 12, pp. 7733–7745, Dec. 2011.

[15] A. Osmane and J.-C. Belfiore. (2011). "The compute-and-forward protocol: Implementation and practical aspects." [Online]. Available: https://arxiv.org/abs/1107.0300

[16] A. Sakzad, J. Harshan, and V. Emanuele, "Integer-forcing MIMO linear receivers based on lattice reduction," *IEEE Trans. Wireless Commun.*, vol. 12, no. 10, pp. 4905–4915, Oct. 2013.

[17] D. Slepian and J. K. Wolf, "Noiseless coding of correlated information sources," *IEEE Trans. Inf. Theory*, vol. IT-19, no. 4, pp. 471–480, Jul. 1973.

[18] R. Storn and K. Price, "Differential evolution—A simple and efficient heuristic for global optimization over continuous spaces," *J. Global Optim.*, vol. 11, no. 4, pp. 341–359, 1997.

[19] O. Ordentlich and U. Erez, "A simple proof for the existence of 'good' pairs of nested lattices," *IEEE Trans. Inf. Theory*, vol. 62, no. 8, pp. 4439–4453, Aug. 2016.

[20] A. S. Avestimehr, S. N. Diggavi, and D. N. C. Tse, "Wireless network information flow: A deterministic approach," *IEEE Trans. Inf. Theory*, vol. 57, no. 4, pp. 1872–1905, Apr. 2011.

[21] C. Feng, D. Silva, and F. Kschischang, "An algebraic approach to physical-layer network coding," *IEEE Trans. Inf. Theory*, vol. 59, no. 11, pp. 7576–7596, Nov. 2013.

[22] H. Cheng, X. Yuan, and Y. Tan, "Compute-compress-and-forward: New results," in *Proc. IEEE Globecom*, Singapore, Dec. 2017, pp. 1–6.

[23] J. Lee, *A First Course in Combinatorial Optimization* (Cambridge Texts in Applied Mathematics), vol. 36. Cambridge, U.K.: Cambridge Univ. Press, 2004.

[24] P. Gupta, G. Kramer, and A. J. V. Wijngaarden, *Advances in Network Information Theory*. Boston, MA, USA: AMS, 2004.

[25] R. Zamir, S. Shamai (Shitz), and U. Erez, "Nested linear/lattice codes for structured multiterminal binning," *IEEE Trans. Inf. Theory*, vol. 48, no. 6, pp. 1250–1276, Jun. 2002.

[26] T. M. Cover and J. A. Thomas, *Elements of Information Theory*, vol. 2, 2nd ed. Hoboken, NJ, USA: Wiley, Jul. 2006.

[27] Z. Liu, S. Cheng, A. D. Liveris, and Z. Xiong, "Slepian-wolf coded nested lattice quantization for Wyner–Ziv coding: High-rate performance analysis and code design," *IEEE Trans. Inf. Theory*, vol. 52, no. 10, pp. 4358–4379, Oct. 2006.

[28] T. M. Cover, "A proof of the data compression theorem of Slepian and Wolf for ergodic sources (Corresp.)," *IEEE Trans. Inf. Theory*, vol. 21, no. 2, pp. 226–228, Mar. 1975.

[29] C. Mobile, "C-RAN: The road towards green RAN," ver. 2.5, China Mobile Res. Inst., White Paper, Oct. 2011.

[30] Y. Zhou and W. Yu, "Optimized backhaul compression for uplink cloud radio access network," *IEEE J. Sel. Areas Commun.*, vol. 32, no. 6, pp. 1295–1307, Jun. 2014.

[31] S.-H. Park, O. Simeone, O. Sahin, and S. Shamai (Shitz), "Joint decompression and decoding for cloud radio access networks," *IEEE Signal Process. Lett.*, vol. 20, no. 5, pp. 503–506, May 2013.

[32] E. Jones *et al.*, *SciPy: Open Source Scientific Tools for Python*. Accessed: Nov. 23, 2016. [Online]. Available: http://www.scipy.org/

[33] S. Fujishige, *Submodular Functions and Optimization* (Annals of Discrete Mathematics). New York, NY, USA: Elsevier, 2005.

Hai Cheng received his B.Eng degree in 2015 from Xidian University, China, and master degree in 2018 from ShanghaiTech University, China. He will pursue his Ph.D. degree in Department of Electrical and Computer Engineering at Northeastern University. His research interests include wireless communication, physical-layer network coding, and optimization.

Xiaojun Yuan received the Ph.D. degree in electrical engineering from the City University of Hong Kong in 2008. From 2009 to 2011, he was a Research Fellow with the Department of Electronic Engineering, City University of Hong Kong. He was also a Visiting Scholar with the Department of Electrical Engineering, the University of Hawaii at Manoa, from 2009 to 2010. From 2011 to 2014, he was a Research Assistant Professor with the Institute of Network Coding, The Chinese University of Hong Kong. From 2014 to 2017, he was an Assistant Professor with the School of Information Science and Technology, ShanghaiTech University. He is currently a Professor with the National Key Laboratory of Science and Technology on Communications, University of Electronic Science and Technology of China, supported by the Thousand Youth Talents Plan in China. His research interests cover a broad range of wireless communications, statistical signal processing, and information theory including multi-antenna techniques, network coding, cooperative communications, and compressed sensing. He has authored over 100 peer-reviewed research papers in the leading international journals and conferences, and has served on a number of technical programs for international conferences. He was a co-recipient of the Best Paper Award of the IEEE ICC 2014. He is an Editor of the IEEE TRANSACTIONS ON COMMUNICATIONS.

Yihua Tan received the B.Eng. degree in 2013 from Zhejiang University, China, and the Ph.D. degree in 2017 from The Chinese University of Hong Kong (CUHK). His research interests include wireless networks, physical-layer network coding, signal processing, software-defined radio, Internet of things, etc.